ISTANBUL TECHNICAL UNIVERSITY ★ INFORMATICS INSTITUTE

TWO-PHASE BLOOD FLOW MODELLING FOR DEEP VEIN THROMBOSIS

M.Sc. THESIS

Utkan ÇALIŞKAN

Computational Science and Engineering

Computational Science and Engineering

Thesis Advisor: Prof. Dr. M. Serdar Çelebi

JUNE 2017

ISTANBUL TECHNICAL UNIVERSITY ★ INFORMATICS INSTITUTE

TWO-PHASE BLOOD FLOW MODELLING FOR DEEP VEIN THROMBOSIS

M.Sc. THESIS

Utkan ÇALIŞKAN
(702151017)

Computational Science and Engineering

Computational Science and Engineering

Thesis Advisor: Prof. Dr. M. Serdar Çelebi

JUNE 2017

İSTANBUL TEKNİK ÜNİVERSİTESİ ★ BİLİŞİM ENSTİTÜSÜ

DERIN VEN TROMBOZU ICIN IKI FAZLI KAN AKISI MODELLEMESI

YÜKSEK LİSANS TEZİ

Utkan ÇALIŞKAN
(702151017)

Hesaplamalı Bilim ve Mühendislik Anabilim Dalı

Hesaplamalı Bilim ve Mühendislik Programı

Tez Danışmanı: Prof. Dr. M. Serdar Çelebi

HAZIRAN 2017

Utkan ÇALIŞKAN, a M.Sc. student of ITU Informatics InstituteEngineering and Technology 702151017 successfully defended the thesis entitled "TWO-PHASE BLOOD FLOW MODELLING FOR DEEP VEIN THROMBOSIS", which he/she prepared after fulfilling the requirements specified in the associated legislations, before the jury whose signatures are below.

Thesis Advisor :	**Prof. Dr. M. Serdar Çelebi** Istanbul Technical University	.....
Jury Members :	**Prof. Dr. M. Serdar Çelebi** Istanbul Technical University	.....
	Assoc. Dr. Mehmet Şahin Istanbul Technical University	.....
	Assoc. Dr. Mine Çağlar Koc University	.....

Date of Submission : **05 May 2017**
Date of Defense : **05 June 2017**

To my family,

FOREWORD

I would like to thank my supervisor Prof. Dr. M. Serdar Çelebi for his endless encouragement and guidance in science and engineering from very first level to the end during my whole MSc study. I would like to thank Assoc. Dr. Mehmet Şahin for showing me the importance and the meaning of computational fluid dynamics in the first place which is the basis of this thesis.

I also would like to thank Samet Demir for his help at the computational lab that made me proceed properly with ths thesis and for being ready to help anytime.

June 2017

Utkan ÇALIŞKAN
(MSc Student)

TABLE OF CONTENTS

Page

ABBREVIATIONS

CVD	**:** Cardiovascular Diseases
VTE	**:** Venous Thromboemlosim
DVT	**:** Deep Vein Thrombosis
RBC	**:** Red Blood Cells
WBC	**:** White Blood Cells
PE	**:** Pulmonary Embolism
FSI	**:** Fluid Structure Interaction
WSS	**:** Wall Shear Stress
NO	**:** Nitric Oxide
PDE	**:** Partial Differential Equation
FVM	**:** Finite Volume Method

LIST OF TABLES

Page

LIST OF FIGURES

Page

TWO-PHASE BLOOD FLOW MODELLING FOR DEEP VEIN THROMBOSIS

SUMMARY

One of the most critical region in vessels is where parietal valves are present due to clot and thrombus formation which causes many cardiovascular diseases such as Deep Vein Thrombosis (DVT). In that sense, the most critical blood component is RBCs in vascular system. Unhealty subjects show that RBCs aggregates and becomes gluey increasing its resistance to flow, dynamic viscosity. This incident may lead blood to form clot and thrombus. Therefore, two-phase non-Newtonian flow model is needed in order to simulate the hemodynamics and to observe the aggregation behaviour of RBCs. This study is contributes to literature of Computational Fluid Dynamics (CFD) methods to model blood flow in vascular system by examining two-phase flow for DVT. The aim of this study is to investigate blood flow more realisticly in deep veins by conducting CFD simulations using OpenFOAM, open source CFD software.

A realistic model of blood is correlated after experimental data by implementing a non-Newtonian Carreau-Yasuda viscosity model with the model parameters proposed by Jung et al. Although this model is proposed for three-phase flow, it can be also applied for two-phase model of Red Blood Cells (RBCs), which is the main cause to the non-Newtonian behaviour of blood, and plasma as the continous phase in which RBCs are suspended. This model is implemented in OpenFOAM, open source CFD software, to simulate blood flow. At first, the validation of our numerical model is performed in comparison with experimental data.

After the validation of our numerical model with experimental data, same model is implemented in three deep vein geometries with venous valves parietal such as deceased cusps, wide open valve and valve with small opening. RBCs aggregation, velocity profiles and pressure contours are investigated in these geometries, representation of deep veins with parietal valves.

With the two-phase blood flow modelling, RBCs aggregation becomes traceable in the flow. Therefore, the volume fraction of RBCs in cells over hematocrit ($H\bar{0}.45$) are shown in contours to observe critical regions for DVT models. Additionally, Spatial Wall Shear Stress (SWSSG) Gradient index value is studied in all the simulations of DVT cases. This study investigates the proper WSS based index representation for spatial WSS derivations around the critical regions such as near parietal valve.

DERIN VEN TROMBOZU ICIN IKI FAZLI KAN AKISI MODELLEMESI

ÖZET

Kan akışının hesaplamalı mühendislik uygulamalarıyla incelenmesi uzun zamandır literatürde yer edinmiş ve teknolojinin gelişmesiyle beraber de oldukça yaygınlaşmaya başlamıştır. Kanın içerdiği bileşenlerden ve sahip olduğu kompleks dinamiğinden dolayı Hesaplamalı Akışkanlar Dinamiği ile simüle edilmesi oldukça zorludur. Fakat mühendis ve bilim adamları problemlerine göre yeterli gördükleri yaklaşımı yaparak, kan akışının modellemesini çok da derine inmeden modelleyebilmektedirler. Kanın akış dinamiği; hız, damar genişliği ve yapısı, hematokrit değeri, kayma gerilmeleri ve benzeri birçok parametreye bağlı olarak değiştiği için kan akışı duruma göre değişik yaklaşımlarla modellenebilmektedir. Örneğin, normalde çok fazlı olan kan, geniş atardamarlarda tek fazlı kabul edilerek deneylere uygunluk gösterecek şekilde simülasyonları gerçekleştirilebilmektedir. Fakat kırmızı kan hücrelerinin jelleşmesi, pıhtı oluşumu ve atımı gibi konularda akış analizleri gerçekleştirilecekse modelin mutlaka çok fazlı, en azından iki fazlı, olarak kurulması gerekmektedir.

Damarlardaki en kritik bölgelerden birisi, pıhtı oluşum ve atımı yüzünden ciddi kalp hastalıklarına sebep olan perietal valf bulunduran toplardamarlardır. Bu hastalıklardan en çok karşılaşılanı Derin Ven Trombozudur (DVT). Toplardamarlardaki kanın belirli sebeplerle jelleşmesi ve pıhtı oluşumuna kadar ilerlemesi ciddi olarak insan sağlığını etkilemektedir. Örneğin ufak bir pıhtının toplar damarda bulunması o an için önemli olmazken bu pıhtının akış ve dış etkenlerle kan yolu boyunca ilerlemesi ölümcül hastalıklara (DVT) yol açabilmektedir. Bu durum kırmızı kan hücrelerinin kan içindeki dinamiğine bağlı olarak oluşmaktadır ki bu tür hastalıklarda inceleme için kandaki en kritik bileşen kırmızı kan hücreleri denilebilir. Doktorlar, erken teşhis çalışmalarında hastanın geçmiş sağlık durumuna ve yaşam tarzına bağlı olarak yaptıkları testlere göre hastanın bu hastalığa sahip olma riskini tespit etmeye çalışmaktadırlar. Bunun yanında sağlıksız bireylerde yapılan teşhislerde kırmızı kan hücrelerinin bazı bölgelerde toplanarak jelleştiği ve viskozitesinin arttığı da görülmüştür. Genel olarak toplardamarda görülen bu durum pıhtı oluşumunun sonucu olarak DVT gözlenmektedir. Bu tez ise DVT tespitinin, geçmiş sağlık durumu ve gündelik yaşantı testleri yerine bilgisayar ortamında gerçekçi kan akışı modeli kurarak gerçekleştirilen simülasyonlara göre yapılmasını amaçlamaktadır. Bu tespitin yapılabilmesi için öncelikle kan akışı modelinin toplardamardaki kan akış dinamiğine uygun olması ve en azından iki fazlı (plazma ve kırmızı kan hücreleri) olarak kurulması gerekmektedir.

Bu çalışmada, kanın derin venozdaki akışının bilgisayar ortamında, Hesaplamalı Akışkanlar Dinamiği (HAD) yöntemleri ile simüle edilerek gözlenmesi amaçlanmıştır. Birçok hastalığa sebep olan pıhtı atımının gerçekleştiği bu toplardamarlardaki akışın incelenmesi, hastalıkların erken teşhisi açısından önem arz etmektedir. Bu damarlarda kanın düşük hızlarda hareketinden dolayı Kırmızı Kan Hücrelerinin jelleşme meyilimi

diğer damarlara göre daha yüksektir. Bunun da sebebi kanın akış dinamiğinin kayma oranına ve hematokrit değerlerine göre değişmesidir. Aynı zamanda valf mekanizmasına sahip bu damarlarda, valf kapakçıklarının arkasında kırmızı kan hücrelerinin yoğunlaşması olasıdır. Bu durumlar değerlendirildiğinde hastanın damar yapısına göre yapılan HAD uygulamaları, o bölge hakkında kapsamlı bilgi sağlayabilmektedir. Fakat bunun için HAD modelinin gerçekci yaklaşımla kurulması gerekmektedir. Valf mekanizmasından dolayı katı sıvı etkileşim modeli, kırmızı kan hücrelerinin yoğunluğunun öneminden dolayı iki fazlı non-Newtonian akış modeli ve damar duvarlarının kas kasılmalarına göre hareketinin de gözlemlendiği birleştirilmiş HAD modeli bu bölgelerdeki erken teşhis çalışmaları için yeterli olduğu söylenebilir. Fakat bu tezde, katının hareketi hesaba katılmadan, iki fazlı non-Newtonian akışkan modeli kurularak sabit hızda HAD simülasyonları gerçekleştirilerek kan akışı gözlemlenmiştir. Fazlar arasında yüzey gerilmeleri dikkate alınmadan fazların tamamen karışım halinde bulunduğu yaklaşımıyla, fazlar arası yüzey gerilmesinin hesaplanmadığı HAD simülasyonları gerçekleştirilmiştir.

Non-newtonian iki fazlı kan akışında, kırmızı kan hücrelerinin viskozitesi için deneysel datalarla korele edilmiş modifiye Carreau-Yashuda modeli kullanılırken plazma fazı için de Newtonian yani sabit viskoziteli akışkan modeli kullanılmıştır. Bu modelde non-Newtonian akışkan fazın viskozitesi, karışım halindeki akışkandaki kendi hacim oranına ve bu fazın kayma oranına göre değişmektedir. Modeldeki denklemler, bir takım deneysel çalışmaların sonuçlarıyla korelasyon yapılarak kurulmuştur. Kırmızı kan hücreleri viskozite modeli için literatürden alınan, aslında üç fazlı kan akışı için tanıtılan modifiye Carreau-Yashuda modeli iki fazlı akış için de uyarlanabilmektedir. Bu model düşük kayma oranlarındaki kan akışı için uygun bir yaklaşım vermekle beraber hematokrit değerine bağlıdır. Bütün simülasyonlar açık kaynaklı OpenFOAM yazılımı kullanılarak gerçekleştirilmiştir. Normalde, iki fazlı karışım teorisi kullanılarak gerçekleştirilen simülasyonlarda non-Newtonian viskozite modeli bulunmadığı için kırmızı kan hücresi için kurulan non-Newtonian modeli OpenFOAM'ın kütüphanelerine sonradan eklenmiştir. Yeni bir model olduğu için eklenen viskozite modeli ile yapılan kan akışının doğruluğu deneysel verilerle kıyaslanarak doğrulama çalışmaları gerçekleştirilmiştir.

İlk önce, OpenFOAM yazılımında kurulan bu modelimizin literatürde deney sonuçları bulunan bir mikro kanaldaki kan akışı çalışmasıyla kıyaslaması yapılarak doğruluğunun derecesi gösterilmiştir. Mikro kanalda yapılan deney sonucuna göre numerik modeldeki hız profilleri aynı grafikte karşılaştırılarak gösterilmiştir. OpenFOAM'da elde edilen sayısal sonuç, mikro kanal deney verisiyle oldukça yakın eşleşme göstermiştir. Ikinci doğrulama çalışması için ani genişleme çemberinde yapılan bir kan akışı deney düzeneği baz alınarak OpenFOAM'da kan akış simülasyonu gerçekleştirilmiştir. Bu modelde de deney bilgileri oluşan büyük vorteks merkezinden dik eksenel çizgi üstündeki hız değerlerin bilgisini vermektedir. Sayısal modelimizin sonuçlarına göre aynı çizgi üstündeki değerler, deney verileriyle kıyaslanmıştır. Bu model için de sayısal sonuçlar deneysel verilerle oldukça uyumlu görülmüştür. Doğrulama çalışmaları, modelimizin deneylere eş sonuçlar verdiği ve kan akışı için uygun bir iki fazlı akış modeli olduğunu göstermektedir. Kan akışının düşük ve orta hızlarda fiziğini ortaya koyan bu model ile aynı zamanda iki fazlı olduğu için kırmızı kan hücrelerinin yoğunluğunun arttığı bölgeler de tespit edilebilmektedir. Hızın ve local hematocrit değerlerinin etkilediği kırmızı kan hücrelerinin viskozitesine

bağlı olarak değişen yoğunluk iki fazlı kan akışı modellemesiyle zamana bağlı olarak gözlenebilmektedir.

Doğrulama çalışmasından sonra DVT incelemesi için üç boyutlu, valfli toplardamar geometrisinde aynı akış modeli kullanılarak simülasyonlar gerçekleştirilmiştir. Bunun için fonksiyonu bozuk valf modeli, fonksiyonel geniş valf açıklıklı ve dar valf açıklıklı model olmak üzere üç ayrı geometride simülasyonlar gerçekleştirilmiştir. Normalde, pulsatif kan akışına göre açılıp kapanan valf mekanizmasının modellenmesi oldukça zor olduğu için, valf konum ve durumuna göre değişken simülasyonlar gerçekleştirerek kıyaslamalar yapılmıştır. Geometrilerin hücresel ağ yapısı delaunay algoritması ile Icem CFD yazılımda oluşturulmuştur. Aynı zamanda geometrinin bazı sınırlarında, örneğin valf kapakçıklarında, prizma hücreler kullanılmıştır. Kırmızı kan hücrelerinin duvardaki davranışını daha iyi tespit edebilmek için prizma hücrelerin kullanılması sonuçların doğruluğu açısından önemlidir. Hızın duvara yakın bölgelerde düşük olması beklendiği için prizmatik hücreler duvara tabaka olarak işlenerek, akış alanının ağ yapısı kurulmuştur.

Bu geometrilerde hız ve basınç profillerinin yanında kırmızı kan hücrelerinin kayma oranı ve hacimsel oranları da gözlemlenmiştir. İki fazlı akış modellemesi sayesinde kırmızı kan hücrelerinin yoğunluğunun arttığı kritik bölgeler tespit edilebilmektedir. Aynı zamanda zamana bağlı olarak artan kırmızı kan hücrelerinin yoğunluğu da gözlemlenmiştir. HAD analizlerinin sonuçlarının görselleştirilmesi Paraview yazılımı kullanılarak yapılmıştır. Bunun yanında valfin başlangıcından yukarı doğru artarak alınan noktalardan geçen çizgiler için hız ve hacimsel oran değerleri grafiklere çizdirilmiştir. Üç boyutlu görselleştirme ve iki boyutlu grafikler, kırmızı kan hücrelerinin yoğunluğunun zamanla valf kapakçıklarının duvar ve arka bölgesinde arttığını göstermektedir. Bunun yanında valf geometrisi ve akışın açıklıktan akmasından dolayı valfin üst-arka bölgesinde geriye doğru bir akış görüşmektedir. Bu geri akış da kırmızı kan hücrelerinin toplanmasına sebep olacak bir etkendir. Aynı şekilde viskoziteyi etkileyen düşük kayma oranları da aynı bölgede görülmektedir. Bundan yola çıkarak, valf kapakçıkları açılıp kapanma mekanizması ile çalışmasına devam ederken kırmızı kan hücrelerinin valf yakınlarında toplanması olasıdır. Bu statis noktalarındaki hareketi de aslında, sağlıklı damarda, valfin hareketinin damar duvarını etkilemesiyle ve ya daha etkili olan kas kasılmasının damar duvarını hareket ettirmesi ile sağlanmaktadır.

Bunun yanında kırmızı kan hücrelerinin toplanacağı kritik bölgeleri tespit etmek için Duvar Kayma Gerilmesi (WSS) ve bu gerilmelerin uzayda değişim değerleri (SWSSG) de gözlemlenmiştir. Bu değerler kanın duvara yakın bölgelerindeki akış durumu hakkında bilgiler vermektedir. Normalde yüksek WSS ve SWSSG değerleri kan damarı için tehlikeli olduğu halde, DVT çalışmasında bu değerlerin düşük olduğu bölgeler daha kritik olmaktadır. Çünkü bu değerlerin düşüklüğü duvardaki o bölgede hareketliliğin az olduğunu ifade eder. Hareketliliğin az olması da kırmızı kan hücrelerinin yoğunlaşmasına imkan sağlamaktadır. Bundan dolayı, bu tarz değerlerin DVT çalışmasıyla bağdaştırılarak yapılan kanıtsal değerlendirmeler ile tez çalışmamız literatüre katkıda bulunmaktadır. Bunlara benzer diğer değer çalışmaları, özellikle zamana bağlı olarak kurulmuş değerler de yine kanıtsal olarak kan damarı içindeki tromboz oluşumuna dair bilgiler verebilmektedir. Iki fazlı akış modelimizle yapılan simülasyonlarda bu değerler de hesaplanarak pıhtı oluşumu hakkında daha kapsamlı bilgi alınabilir. Bu sayede, kan akışının iki fazlı ve özel viskozite modeliyle simüle

edilmesi ve akış sonuçlarına göre hesaplanan değerler ile beraber olası pıhtı oluşumu hakkında önceden tespit yapmak mümkün olmaktadır.

1. INTRODUCTION

There are huge enthusiasm and several research activities centered today on the investigation of blood flows. According to American Heart Association, Cardiovascular diseases (CVDs) are the leading cause of death in the US, and contribute more than three hundred billion dollars annually to the national health care cost. Therefore Venous thromboembolism (VTE), including Deep Vein Thrombosis (DVT) and pulmonary embolism, affects assumedly 71 per 100,000 persons yearly [1]. In 2005, the House of Commons Health Committee [2] reported that every year an approximated 25,000 people in the UK die from avoidable hospital acquired VTE. This comprises patients entered to hospital for medical care. The inconsistent use of prophylactic measures for VTE in hospital patients has been widely reported such that A UK survey suggested that 71% of patients assessed to be at medium or high risk of developing DVT did not gain any mechanical or pharmacological VTE prophylaxis [3].

Approximately one third of patients with VTE have a pulmonary embolism, whereas two thirds have DVT alone [4]. DVT causes thousands of hospitalizations with the ratio of per death out of 5 hospitalizations. Although it is the most preventable disease in hospitals, it is one of the third most common cardiovascular disease. Moreover, reports shows that the number of hospitalizations ranged from 300,000 to 600,000 in 1990?s where the number of death caused by DVT is 50,000 per year [5]. The incidence rate of isolated deep venous thrombosis, from 9 population based studies, is around 50 per 100,000 person-years [6]. Furthermore a study in Massachusetts evaluated that an occurrence of pulmonary embolism, with or without DVT, is 23 per 100,000 and an occurrence rate of DVT only is 48 per 100,000 person-years [7]. The occurrance rate of pulmonary embolism is challenging to quantify, however, as it is often not diagnosed without autopsy.

Computational fluid dynamics (CFD) is widely used to simulate complex blood flow in complex geometries such as deep veins with valve mechanism. The challenging part is to investigate blood flow is its complex dynamics which has to be modelled.

Many computational approaches have been conducted to investigate realistic blood flow [8–10] Since blood consist of many phases such as plasma %55 and %40 Red blood Cells (RBCs), %2 White Blood Cells (WBCs) and %2 small blood components dispersed in Newtonian plasma, dynamics of multiphase blood flow can be defined with different approaches. In this thesis, Mixture Theory is used to consider blood as two-phase fluid, RBCs suspended in plasma. High number of RBCs as small particles in blood leads the flow exhibit non-Newtonian behaviour. Since RBCs (e.g. %40) behave as non-Newtonian fluid in blood, one-phase non-Newtonian flow approaches would not be really efficient way to simulate blood flow in deep veins where blood flow is slow and shear rates are significantly small. Moreover the concentration of RBCs contributes to blood clotin in vein which then may cause fatal situation. Therefore modelling of RBCs apart from plasma is crucial. Since RBC concentration is crucial in deep veins, we considered a two-phase Eulerian-Eulerian CFD model where plasma is Newtonian fluid and RBCs are non-Newtonian fluid. Model Description is such that the two-phase non-newtonian CFD model where one phase (RBCs) is dispersed in other phase (plasma). Model geometries for DVT cases represent an actual deep vein geometry which is obtained from a human body. The numerical model is established in OpenFOAM, open source CFD software with many numerical methods hardcoded inside in order to model dispersed phases. We have modelled RBCs viscosity model due to volume fraction and shear thinning in order to capture hemodynamics properties of blood flows. There are many mathematical methods which have a constitutive equation due to shear rates plus to Navier-Stokes equation are developed to investigate the hemodynamics of blood flow [11, 12].

Multiphase approach for blood flow requires to solve Navier-Stokes equations for each phase and constitutive equations as the mechanism between the phases for momentum exchange, heat and mass transfer. In this paper, the two-phase model defines different phases as inter-penetrating continua. This thesis presents several 3D simulations of blood flow using advanced non-Newtonian blood viscosity model in a deep vein to estimate the potential stasis conditions by RBC aggregation. The early diagnosis of DVT is crucial as it could keep patient from happening a pulmonary embolism (PE) which could be causing end of life. However, due to the limitations of computational

studies, two-phase blood flow modelling, RBCs dispersed in plasma, is presumed to be sufficient to observe realistic blood flow in terms of the diagnosis of DVT.

The main purpose of the computational study on multi-phase blood flow is to diagnose possible blood clot formation in risky regions such as parietal values of the deep vein. Realistic modelling of blood flow in DVT will provide better understanding of how blood clot forms along with valve mechanism. In this study, instead of Fluid-Structure Interaction (FSI) between blood and valves, several cases with different valve opening angles are studied. Therefore, several parameters which would influence the blood clot formation will be examined in detail. Mostly, Wall Shear Stress (WSS) and its spatial derivation will be studied.

In the second chapter, the literature on blood flow is reviewed. This chapter discusses the importance of the proper blood flow in the vessel, critical diseases particularly DVT and other such properties of the veins in order to better understand several phenomena which happen in deep veins. Significance of the computational study on blood flow is also pointed out as an important factor in medicine as well as the diagnosis of such phenomena.

In the third chapter, the methods and numerical approaches for modelling blood are discussed as well as the equations to define RBCs viscosity for two-phase blood flow.

In the forth chapter, CFD cases are presented. The validation of the numerical model in OpenFOAM is also indicated with a micro-channel geometry and a sudden expansion channel benchmark. For DVT cases, several deep vein geometries due to their valve positioning are presented.

The fifth chapter exhibits the result of the numerical simulations for several cases of DVT with the velocity and the pressure profiles as well as wall shear stress. Additionally, the index value which is based on WSS is also demonstrated in the chapter. In order to predict the potential DVT, WSS based index called Spatial Wall Shear Stress gradient is presented and critical importance is showed.

2. LITERATURE REVIEW

In this chapter, the literature on veins's properties, valve's functionality, possible cardiovascular diseases in deep veins and the importance of blood flow modelling are reviewed.

2.1 Deep veins, Venous valves and Deep Vein Thrombosis

Veins carry blood from all the body organs to the heart. The large veins parallel the large arteries and often share the same name, however, the lane of the venous system are more complicated to trace than the arteries. Plenty of unnamed small veins form random networks and join with the large veins. 64% of our blood is carried in the veins. Moreover, veins can expand to hold large amounts of blood. Some veins, specifically those in the arms and legs, have one-way valves to control the blood flow.

The venous valves are really small and delicate. They are present in the blood veins and they have two flaps.These venous valves are bicuspid flap like form made of elastic tissue. The valves function to keep blood moving in one direction. Venous valves have an important function of eliminating the reverse flow of the blood in the veins to remain their work efficaciously and thus the venous valves are considered crucial for the circulatory system. They keep the flow one-way by regulating it against the gravity and even if vacuum pressure gradient is present. Each valve consists of two flaps which is simulated in this thesis (cusps or leaflets) with edges that meet. Shapir and Lev have stated that the cusps of the venous valves consist of thin collagen half-moon-shaped folds covered by endothelium, which originate from the wall of the vein proximate to each other [13]. The cusps' bases where they join the vein wall are thicker. This thickened connection of the cusp is generally called as *limbus* or *tuberculum*. Furthermore, incompetent valves in deep veins cause venous pressure increases and reverse blood flow which then develops venous pathology. Unending venous issue may likewise come about because of venous deterrent or a mix of both valve inadequacy and impediment. These instruments serve to create both global or

local venous hypertension, especially with standing or strolling [14]. Decent and disordered veins with valves are shown in Figure 2.1. Lane et al. [15] has stated that disordered venous valves cause venous hypertension in most cases by reflux through valves.

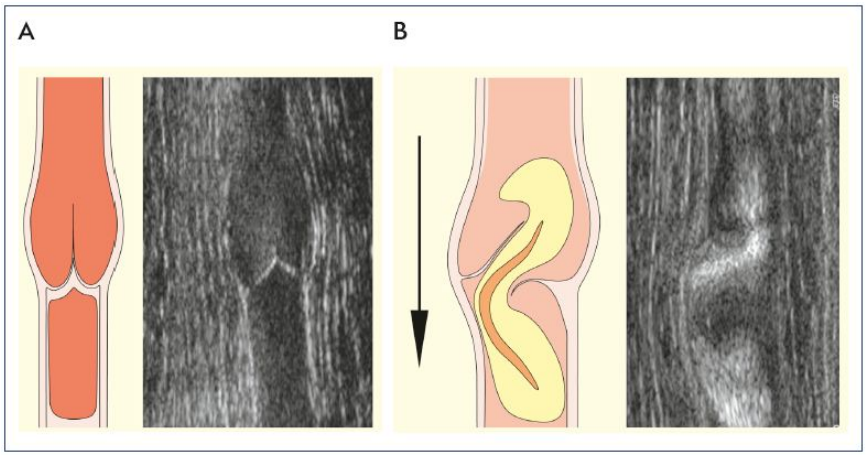

Figure 2.1 : Illustration and visualization of operative (A) and disordered (B) venous valves, the photo from [15] .

The blood flow moving toward the heart, lifts the cusps open like a pair of one-way fluctuating string. If gravity or muscle contractions try to draw the blood backward or if blood begins to regress in a vein, the cusps are back to closed, preventing backward flow. Therefore, valves help the recovery of blood cycle by opening when the blood moves to the heart and closing to the possibility of blood to flow backward because of gravity. Moreover, when the muscles wrapping the deep veins compress them, helps to force the blood toward the heart. The deep veins exist in the lower body and they help channel the blood through the veins from the lower extremities. The deep veins which are present in the leg are wrapped well by the muscle and are supported by the tissue enclosing them. 90-95% of the venous outflow from the leg occurs by these veins [16].

Blood clot(thrombus) which is formed in the deep veins of the body, especially in the legs, causes DVT. DVT may cause swelling or pain in the leg, however, may also occur without any symptoms. DVT or pulmonary embolism (PE) which prevail crucial factor of morbidity and mortality, are the expressions of venous thromboembolism (VTE) and those may occur after surgery and trauma when extended immobilization of the lower limb is needed [17].

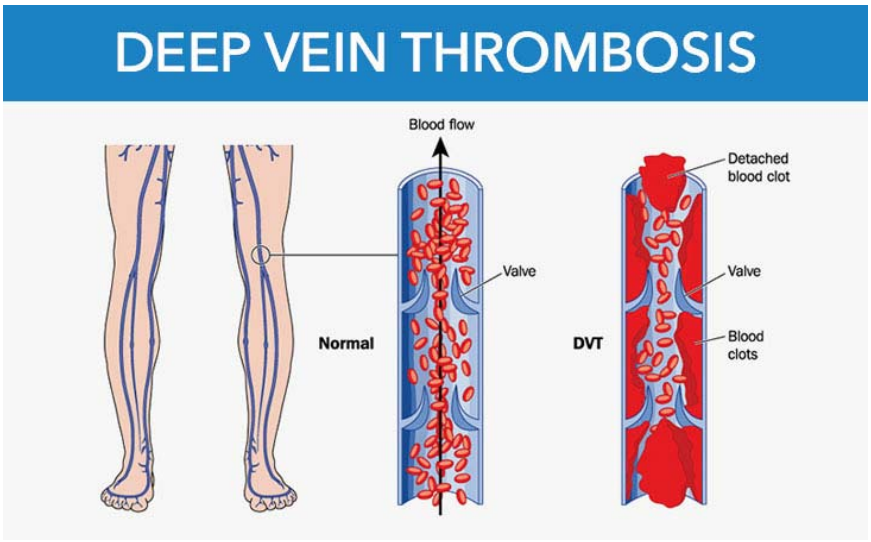

Figure 2.2 : Illustration of DVT from [18] .

The blood flow in deep veins is complex for various reasons such as the low pressure in the veins, irregular flow rates from nearly no flow during quiet sitting or standing positions to high during muscle compressing, the gravity force, the nature of the venous wall as collapsable, the venous valves, and the big volume of blood carried in the deep veins.

Once the blood has gone by the arteries through the capillaries, it flows at a slower rate as little pressure remains to force the blood move forward. Blood flow in deep veins is also pushed back up to the heart by the muscle compression. The walls of the veins are loose and thin and thus many veins are located in the muscles to compensate this. Movement of the leg squeezes the veins, which pushes the blood toward the heart. When the muscles contract the blood within the veins is squeezed up the vein and the valves open. This is indicated as the muscle pump. When the muscle is at rest, as usual, the valves close to prevent the backward blood flow.

Thrombosis occurs if normal homeostatic balance is disturbed. In health, clots do not present in blood, however, the rapid formation of a solid plug occurs to repair the injury of the blood vessels which is indicated as normal homeostasis. The presence of a clot within the non-damaged vascular system such as deep veins causes thrombosis which is a pathological process. This means a pathologic extension of normal homeostasis. The people who undergo various types of surgery are at high risk of having venous thromboembolic disease. DVT commonly causes immobilization, trauma, obesity, malignancy, cardiac disease and stroke. Virchow [19] was the first to summarize the factors of influencing thrombus formation such as alterations in blood flow, vessel wall damage, blood hypercoagulability. Changes in blood flow (e.g. venous stasis) have been shown to grow the risk of thrombosis. Stasis of the blood can occur in states of immobility when the blood is allowed to pool in the intramuscular sinuses of the calf that become stretched during prolonged bed rest. Autopsy studies have showed that the prevalence of DVT is high in patients confined to bed for a week or more prior to death [20]. Patients are exposed to these same risks when confined to bed either before or after surgery. Elderly, bedridden patients, especially those with varicose veins and incompetent valves have a tendency to suffer from venous dilation in the legs, and this can also lead to venous pooling and stasis. Venous obstruction is another cause of stasis as in patients with pelvic tumors or proximal vein thrombosis. It can be said that when blood flow decelerates, there is more time for the accumulation of clotting factors. Moreover, formed small thrombi can not be washed away if there is inadequate flow. Hence, venous stasis is often correlated with DVT. Coagulability can be affected by changes in the blood itself and thus boost thrombus formation. With increasing age, blood coagulability increases. Changes in blood coagulability also occur secondary to a variety of medical conditions [21]. Additively ,when the endothelium of a vessel is injured, platelet adhesion, revealing the subendothelium to blood and aggregation are triggered and tissue factor is activated, which promotes blood coagulation.

2.2 Computational Studies

Computational Fluid Dynamics (CFD) methods have become a significant role to study blood flow. Investigating blood flow by CFD is proven to be practical, reliable and efficient due to the advantage of low cost and simplicity of testing different

physiological conditions. Since the factors such as blood rheology, physiological flow conditions, interactive forces between phases, mechanical properties of blood vessels influence the performance of CFD models. Therefore it is significant to model proper blood rheology for CFD simulations. Firstly, blood viscosity and physiological conditions are clarified by studies to integrate the results obtained by experimental data into CFD models. Cho and Kensey [22] has introduced some hemorheological models in their studies. With the advancement in hardware and software technology, computational methods, medical imaging technology increased the importance of CFD in blood flow modelling. The blood flow modelling started with Newtonian fluid approach in averaged artery geometries, later, included non-Newtonian approach together with genuine artery geometries. More realistic models have been presented including the image-based CFD models in realistic arterial geometries [23], multiphase CFD models based on Euler-Euler approaches [24] and Euler-Lagrangian approaches [25] and also Fluid Structure Interactions with pulsative flow [26].

Many experimental studies has shown that blood flow holds non-Newtonian behaviour such as viscoelasticity, shear thinning, yield stress and thixotropy. Tomiyama et al. indicated the influence of plasma viscosity on blood rheology [27]. Chien presented the effect of RBC aggregation and deformability [28]. Moreover it is indicated that blood rheology is affected by hematocrit, rate of shear, gender, temperature, lipid loading, cholesterol level [22]. Mainly, the blood viscosity models can be categorized as Newtonian viscosity and non-Newtonian viscosity models.

To investigate the complex hemodynamics of blood flow, researchers have developed mathematical models with constitutive equation depending on the shear rates or the hematocrit [29, 30]. In the large-scale vascular where atherosclerosis would frequently occur, it is suggested that multiphase non-Newtonian CFD model is suitable in order to compute flow hemodynamics of RBCs and plasma for the blood's concentrated suspension flow [31]. RBC is the main factor to affect most of the overall hemodynamics force. Since it is confirmed that the RBCs designate the rheological behaviour of blood, multiphase CFD model is necessary to observe the behaviour of blood which is not possible to examine with single phase CFD model. The multiphase model can be extended to incorporate the blood rheological properties at low shear rates [24].

In the past, different multi-segment models for blood have been produced. For the simulations in which RBCs effect is crucial the Immersed Boundary Method consolidated with the Lattice Boltzmann Method, are helpful techniques in order to examine the complex behaviour of blood or RBCs in smaller scale stream, especially because of the distortion, collection of the RBCs. Although these methods have been useful in demonstration of non-Newtonian behavior of blood, they require high computational cost, hence, restrictive for industrial and engineering simulations [32]. There is another optional technique, which considers fluids as mixture [33], to overcome the restriction of high computational cost yet at the same time provides useful information to predict clot formation in deep veins, such as the volume fraction dispersion of the RBCs. The mixture of blood can be presumed to compose of plasma as Newtonian fluid and RBCs as a shear-thinning fluid. Jung et al has stated the method consist of Eulerian-Eulerian multiphase model of blood flow [31]. Rusche [34] has implemented the mixture theory algorithm in OpenFOAM [35], open source CFD solver written in C++. Moreover, Kim [36] used this model to simulate blood flow.

All these studies help in improving the prophylaxis given to the patient by examining the flow physics in detail by courtesy of the numerical simulations. Also, in some cases, patient specific models are being used to carefully analyze the physics involved. Hence, CFD can be used as a useful non-invasive method to diagnose the DVT in the future.

2.3 Blood Rheology and Compositional Properties of Blood

Fluids are principally relegated into two main types, as follows Newtonian Fluids and Non-Newtonian Fluids. The Newtonian Fluids exhibits a linear cognation between stress and strain and thus the dynamic viscosity coefficient of a Newtonian fluid is not dependent of time or strain rate. On the other hand, fluids in which the cognation between the stress and strain is intricated are called Non-Newtonian. Blood behaves as a Non-Newtonian fluid. The hematocrit and blood components has a big impact on blood viscosity. Frankly, blood viscosity increases with the incrementation of the hematocrit which is shown in Figure 2.3. Additionally, the blood temperature has an effect on its viscosity as there is a consequential increase in the viscosity with a decrementation in temperature. Under laminar flow conditions, the presence of cellular

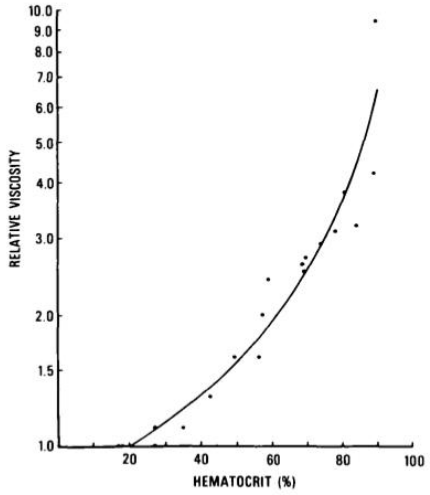

Figure 2.3 : Blood viscosity as a function of hematocrit [37] .

elements disturbing the flow streamlines is the primary reason why blood viscosity is higher than plasma viscosity is.

The entire blood viscosity is the most all around examined property of blood. It demonstrates a Non-Newtonian behaviour with expanding shear rate. Blood viscosity can be characterized as the amount that depicts the blood's resistance to stream, which is being distorted by either shear stress or tensile stress. For various parts of the circulatory framework, diverse behaviours of blood viscosity appear to happen. In salubrious straight immensely colossal blood vessels, where the blood flow is in high strain rate, blood shows Newtonian comportment. However, in diminutive blood vessels, where the strain rate is low, the blood viscosity shows a shear-thinning demeanor. This deportment is expounded by the deformation and aggregation of RBCs. Since blood has many elements suspended inside, RBCs aggregation causes blood thickens at low strain rates. This is known as roulleaux formation [38].

Due to the blood's biological function and effects on hemodynamics, RBCs are the most crucial component in blood. RBCs' main task is to bring oxygen to maintain gas exchange process that mainly occurs in the microvascular network of arterioles, venules and capillaries. RBCs' enzimatically synthesis of nitric oxide (NO) is also indicated recently. The regulation of vascular tonus may be contributed by the exposure of RBCs to physiological levels of shear stress which activates the NO synthases and the export of NO from the RBCs into the blood vessel [39].

RBCs which are eminently deformable particles due to their circular biconcave shapes, constitute around 35-50% of the blood volume in the human body. Geometrically, undeformed RBCs are 7.8 μm in diameter on their circular discoid plane and 2 μm in average thickness on the biconcave radial plane. Their average volume is 90 femtolitre and surface area is about 136 μm2 [40, 41]. RBCs exhibits viscoelastic behaviour and affect the blood flow by their volume fraction which is a significant effect in blood flow. [42].

Furthermore, the viscoelastic rheological features of the RBCs and their volume fraction will progressively impact on blood flow. Moreover, the diameter of vessel has a prevailing role in the blood flow characteristics and the relationships between RBCs in the overall flow stream which may be neglected for vessel diameters larger than 0.2 m [42]. Blood as the fluid medium would be considered as a homogeneous and Non-Newtonian fluid in a continuum concept. [41]. But, in the case of vessels of smaller diameters, for instance arterials, venules and capillaries, the size of RBCs would be relative to the vessels diameter. Therefore, the concept of multiphase blood flow that is described as the suspensions of RBCs in plasma would bring some new questions. Accumulation of the RBCs also has a great importance in abundant biological processes where in the case of human and many other mammals blood, RBCs accumulate at lower shear rates that form linear or fractal-like shapes called Rouleaux [41, 43, 44]. According to the previous studies, the shear rate, haematocrit and the concentration of macromolecules in the plasma (suspending medium) are the key factors effecting the accumulation of blood [45, 46]. Based on pathophysiological point of view, a different state of RBCs accumulation is prevalently obsereved among the patients with peripheral vascular disease in which the high level of accumulation will cause a higher risk of cardiovascular disease. Although, the high level of RBC accumulation level is prevalent after myocardial infraction, ischaemic brain infract, in diabates, and during spesis. Moreover, the RBC accumulation level would be related to cell's deformobility that can differ physicological and pathological states. The RBC deformobility would be different according to their life period in physicological conditions such as parasitic infection, sepsis, diabetes and genetic defects in the RBCs. Based on the aforementioned studies a clear view of the mechanics of RBC accumulation would lead to a better understanding of cardiovascular disease and

the pathology of the blood. Accroding to the general hydrodynamic relationship between RBC accumulation and microclercular blood flow, the RBCs will lead an elevation of blood viscosity thus a resistence to the blood flow. The physiological and pathological important role of RBCs accumulation has brough about some highly extensive experimental studies [28, 41, 43, 44, 47, 48].

It is known that blood behaves as a non-Newtonian fluid in a vessel whose characteristic dimension is about the same size as the characteristic size of blood cells, exhibiting shear-thinning and stress relaxation. Anand et al. [49] has stated that at low shear rates, due to RBC aggregation, blood seems to have a high ostensible viscosity while at high shear rates, due to RBC disaggregation, the opposite demeanor is observed. Yeleswarapu has stated a model which has been able to capture the shear-thinning demeanor of blood over a wide range of shear rates [50]. Moreover, the property of shear-thinning viscosity becomes weaker and eventually disappears as the hematocrit decreases [51]. Experimental data of RBCs viscosity as a function of Shear rate (s^{-1}) is shown in Figure 2.4 by Brooks [51].

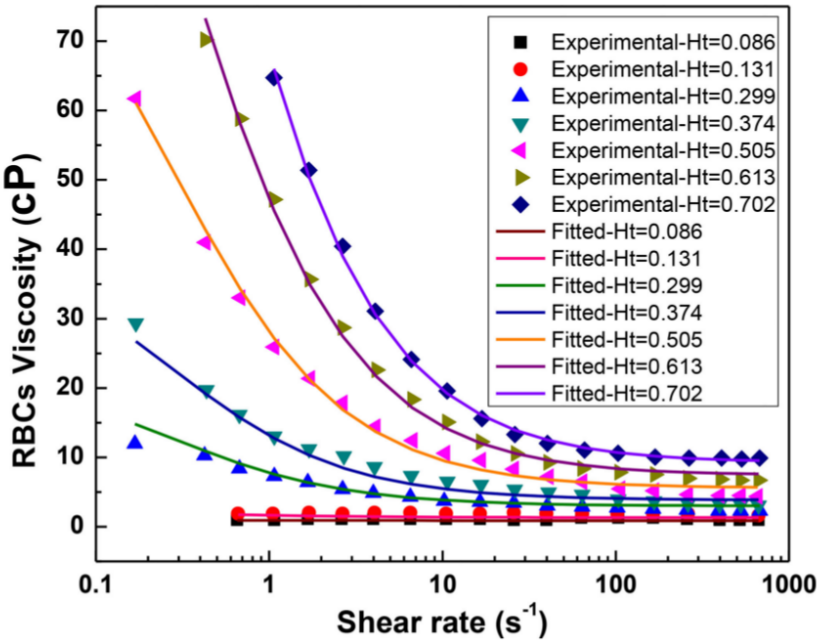

Figure 2.4 : RBCs viscosity due to shear rate, picture from [52].

The fluid flows thorugh pipes or tubes is actually similar to the fluid flow in vascular system due to its homogeneous attribute. Fluid flow is relegated into two types flows which are laminar flow and turbulent flow. In this study, due to blood's low Reynolds number, flow is considered as laminar in the simulations. Laminar flow, is the flow in which the particles of fluid move a zero velocity near the walls and the maximum velocity in the axial stream. Particles in a laminar flow follow the well defined path and thus traceble.

2.4 Wall Shear Stress and Spatial Wall Shear Stress Gradient

Wall shear stress (WSS) is the digressive drag constrain created by blood moving over the endothelial surface. WSS is a function of the velocity gradient of blood close to the endothelial surface. Its extent is specifically relative to blood stream and blood consistency and conversely corresponding to the 3D shape of the span. Along these lines, a little change in the span of a vessel will largely affect wall shear stress. WSS manages blood vessel wall redesigning. Veins grow because of high shear stress.

Amid the advancement of the circulatory framework, blood stream and vascular changes are emphatically coupled. Hemodynamic forces following up on the veins result in a continually evolving geometry, because of the versatility of the vein walls. Of these hemodynamic powers, the WSS has seen a solid increment in consideration in the course of the most recent decade. The endothelial cells that layer the internal wall of veins respond in different approaches to changes in the shear stress, e.g. low shear zones lead to the formation of cilia [53] and the statement of certain development components [54, 56]. These responses are significant in the improvement of the cardiovascular system [55]. The fundamental mechanisms at cellular level, is a theme of current research, see [57, 58]. WSS likewise assumes a part in the etiology of various diseases: for example, areas with low or wavering WSS have been connected to atherosclerosis' the testimony of defenseless plaque at the vein walls [59]. It is well-known that wall shear stress causes vessel dilation in an acute manner.

WSS has a key part in the interaction between blood stream and the encompassing tissue. Velocity measurements with adequate spatial and temporal determination are needed in order to get quantitative data about this parameter.

Blood flow in blood vessel bifurcation sections is of principal significance in comprehension of the biomedical pathophysiology of atherosclerosis. Biomechanical variables, such as, wall shear stress (WSS), spatial wall shear stress gradient (SWSSG), blood consistency and flow velocity might be responsible for the formation and localization of atherosclerosis [60]. High WSS is frequently joined by critical SWSSG. Mathematically, SWSSG is the vector defined as the gradient of the spatial field of WSS. The spatial subordinate of WSS along the stream direction concerning the streamwise distance. Taking after stream impingement at a bifurcation peak, stream that parts into the girl branches encounters fast increasing speed and afterward deceleration, making areas of positive and negative SWSSG, see [61, 63]. Several studies showed that in vivo, cerebral aneurysms start in the quickening zone characterized by both high WSS and positive SWSSG [61–64]. Furthermore, CFD investigations states that high WSS, SWSSG is likewise huge at the throats of stenoses [65, 66]. Insight into how high WSS alone or combined with SWSSG influences endothelial cells function and consequent vessel rebuilding is vital for understanding both ordinary vascular capacity and several pathological developments interceded by hemodynamics.

High WSS and SWSSG are considerably important in physiological and pathological vascular remodeling. This index value is observed to detect the potential clot and thrombosis formation for early diagnosis. In this study, blood flow characteristics are analyzed based on this index and WSS beside the RBC concentration on the critical valve region.

For the subject of DVT, small WSS and SWSSG are critical because of RBCs aggregation. Small stresses on the walls and the small gradient of these stresses, shows that those regions are stagnant. Therefore, small index values which shows the stagnant regions near walls, are observed in this thesis. The equations and calculations of these index values are explained in Chapter 5.

3. MATHEMATICAL MODELLING

In this chapter, mathematical modelling of two-phase blood flow is discussed in detail where momentum and the constitutive equations to be solved, the steps to prepare the model, correlated shear rate viscosity model and critical index values are focused. Moreover it also explains the created meshes for various geometries, applied boundary/initial conditions.

3.1 Governing Equations

In principle, fluid dynamics' equations are composed of the continuity equation which represents the conservation of mass and momentum equations which are known Navier-Stokes equations for fluid dynamics.

Blood is considered as a two-phase mixture, composed of the RBCs dispersed in a plasma. In the absence of thermo-chemical and electromagnetic effects, the governing equations consist of the conservation of mass and momentum equations. For two-phase flow, the equations of conservation of mass are calculated for each phase as well as momentum equations. The equations of conservation of mass in the Eulerian form are, $(f = plasma, d = RBCs)$

$$\frac{\partial \rho_f}{\partial t} + \bigtriangledown . \rho_f v_1 = 0 \tag{3.1}$$

$$\frac{\partial \rho_d}{\partial t} + \bigtriangledown . \rho_d v_2 = 0 \tag{3.2}$$

$$\varepsilon_f + \varepsilon_d = 1 \tag{3.3}$$

where $\frac{\partial}{\partial t}$ is the derivative with respect to time and $\bigtriangledown$ is the divergence operator, ε_f and ε_d represent the volume fraction of phases such as plasma as continuous fluid and RBCs dispersed phase where $0 < \varepsilon_{min} < \varepsilon_{max} < 1$ Each phase occupies exactly the amount of its volume fraction. In this study, ε_d is a function of position and time which also affects viscoelastic behavior of the blood. ε_d is normally a patient based parameter dependent the vivo.

Minor blood components such as white blood cells are neglected and the mixture density of the blood is the average of densities of plasma and RBCs weighted by the volume fractions.

$$\rho_{mix} = \varepsilon_{plasma}\rho_{plasma} + \varepsilon_{RBC}\rho_{RBC} \tag{3.4}$$

The momentum equations for two-phase blood flow is shown below; for plasma:

$$\frac{\partial \rho_f \varepsilon_f v_f}{\partial t} + \bigtriangledown.\rho_f \varepsilon_f v_f v_f = -\varepsilon_f \bigtriangledown p + \bigtriangledown.\hat{\tau}_f + \varepsilon_f \rho_f g + \beta_{fd}(v_d - v_f) + F_f \tag{3.5}$$

for RBCs:

$$\frac{\partial \rho_d \varepsilon_d v_d}{\partial t} + \bigtriangledown.\rho_d \varepsilon_d v_d v_d = -\varepsilon_d \bigtriangledown p + \bigtriangledown.\hat{\tau}_d + \varepsilon_d \rho_d g + \beta_{df}(v_d - v_f) + F_d \tag{3.6}$$

Where ρ is density, p pressure, $\hat{\tau}$ the stress tensor, g the gravity force, F represents the external forces such as virtual mass, lift forces, electricity and magnetism. In order to solve conservation equations, Eqs. 3.1-3.6, additional constitutive relations for the interaction between phases must be defined for blood flow. β is for the interphase momentum exchange coefficients for plasma and RBCs in the drag force.

The constituve equations are categorized for plasma stress tensor and RBC stress tensor. Plasma phase of the blood is considered as Newtonian fluid thus the viscosity is constant. The stress tensor for the plasma phase is shown below,

$$\hat{\tau}_f = \varepsilon_f \mu(\bigtriangledown \overrightarrow{u} + \bigtriangledown \overrightarrow{v})^T + \varepsilon(k - \frac{2}{3}\mu) \bigtriangledown . \overrightarrow{v} \hat{I} \tag{3.7}$$

where ε, k, μ, $\hat{I}$ are volume fraction, bulk viscosity, shear viscosity for the plasma phase and unit tensor, respectively. The stress tensor for the RBCs phase is shown below,

$$\hat{\tau}_d = -p\delta + \varepsilon\mu(\bigtriangledown \overrightarrow{u} + \bigtriangledown \overrightarrow{v})^T + \varepsilon(k - \frac{2}{3}\mu) \bigtriangledown . \overrightarrow{v} \hat{I} \tag{3.8}$$

where δ is Kronecker delta. This parameter is to define the pressure fluctuation due to the collisions of the particles and represents an interparticle pressure as a function of volume fraction of RBCs. The effective and shear viscosities of non-Newtonian fluid represented by k and μ in the equations are dependent on the volume fraction and the shear rate of non-Newtonian phase. Even with the high concentration of the RBCs

(%98 hematocrit), blood still behaves like a fluid. Therefore interparticle pressure for a suitable hematocrit range was negligible.

The model proposed by Jung et al. [24] which defines a shear rate and volume fraction dependent viscosity model, is used in this study. The RBCs are assumed to behave as a viscoelastic shear-thinning fluid, thus the volume fraction is also a parameter of the function which defines the viscosity of blood.

In order to simulate the non-Newtonian shear-thinning behavior of blood, a modification of the Carreau-Yasuda viscosity model presented by Jung et al [24], is used in which the effective RBC shear viscosity, μ_{RBC}, was obtained from the equation of dimensionless relative viscosity, η, of blood mixture for two-phase liquid. This modified Carreau-Yasuda model and its parameters for blood viscosity are determined after the experimental data from Wojnarowski [67] and Brooks [51].

$$\eta = \frac{\varepsilon_{RBC}\mu_{RBC} + \varepsilon_{plasma}\mu_{plasma}}{\mu_{plasma}} = m[1 + (\lambda\dot{\gamma})^2]^{(n-1)/2} \tag{3.9}$$

where m, λ, n are parameters to define blood mixture viscosity and $\dot{\gamma} = \bigtriangledown\overrightarrow{v} + (\bigtriangledown\overrightarrow{v})^T$ is the shear rate. Correlated polynomials for low shear rates are shown in Figure 3.1.

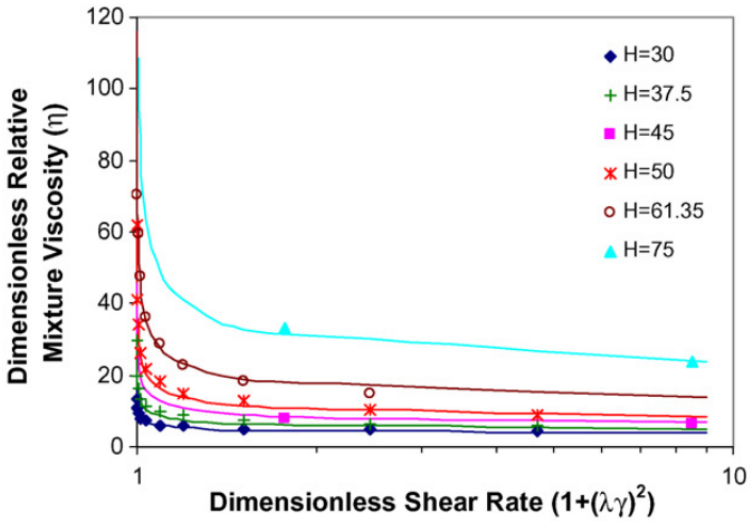

Figure 3.1 : Dimensionless relative blood viscosity versus dimensionless shear rate and hematocrit, experimental data from [51, 67], picture from [24].

The time coefficient, λ, was taken as 0.110 s and the two parameters n and m are the functions of the hematocrit value and the shear rate. The relations of these parameters, for $\dot{\gamma}$ greater than 6, is given by the polynomial approximations below [24];

$$
\begin{aligned}
m &= 0.8092\varepsilon_{RBC}^3 - 0.8246\varepsilon_{RBC}^2 - 0.3503\varepsilon_{RBC} + 1 \\
n &= 122.28\varepsilon_{RBC}^3 - 51.213\varepsilon_{RBC}^2 + 16.305\varepsilon_{RBC} + 1
\end{aligned}
\tag{3.10}
$$

for $\dot{\gamma}$ lesser than 6 at low shear rates;

$$
\begin{aligned}
\frac{(n-1)}{k} &= -0.8913\varepsilon_{RBC}^3 - 2.0679\varepsilon_{RBC}^2 - 1.7814\varepsilon_{RBC} + 1 \\
m &= 70.782\varepsilon_{RBC}^3 + 2.0679\varepsilon_{RBC}^2 + 1.7814\varepsilon_{RBC}0.3503\varepsilon_{RBC} + 1
\end{aligned}
\tag{3.11}
$$

The model, polynomials, are adopted to the experimental data for a wide physiological range of shear rate and hematocrits. This model is quite useful when blood is at low shear rate and determines RBCs viscosity including RBCs agglomeration as a function of the shear rate and the volume fraction of RBCs.

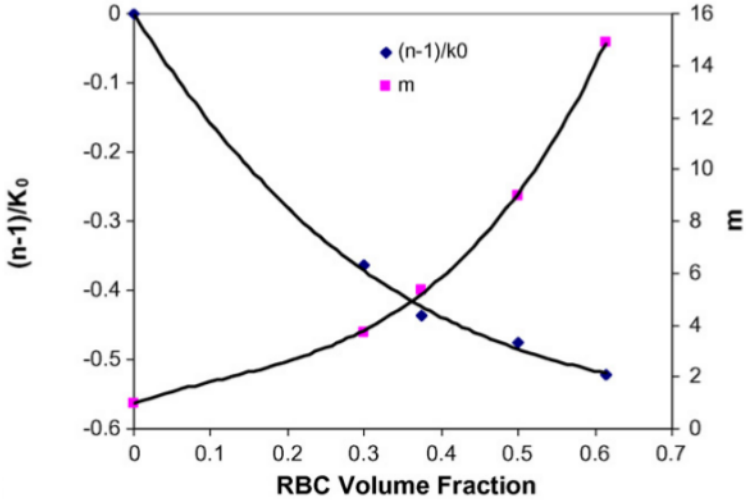

Figure 3.2 : m and n versus RBC volume fraction at low shear rates $(1+(\lambda\gamma)^2 \leq 1.5)$. Experimental data is marked by points at different hematocrits and shear rates, picture from [24].

While mixture fluid moves, two different phase interacts each other. Plasma, RBC interaction brings out the interphase momentum exchange coefficients and the velocity differences between the continuous(plasma) and disperse phase(RBCs). In this study, Schiller and Naumann [68] model is used for the interaction force between the two components. The drag coefficient on a single sphere is,

$$
C_d = \frac{24}{Re}(1 + 0.15Re^{0.687}) \tag{3.12}
$$

and β parameter in the momentum equation (Eq. 5) is as follows,

$$\beta = \frac{3}{4} C_d \frac{\rho_{plasma} \varepsilon_{plasma} \varepsilon_{RBC} |\overrightarrow{v_{plasma}} - \overrightarrow{v_{RBC}}|}{d_{RBC} \phi} \tag{3.13}$$

where d_{RBC} is the diameter of red blood cells and ϕ is the dynamic shape factor.

The drag coefficient calculations can be modified in OpenFOAM to correct limiting behaviour for Re $<$ 1000 as,

$$C_d = 0.44 \quad for \quad Re \geq 1000 \tag{3.14}$$

Drag is affected by the agglomerate nonspherical particles in fluid [69]. However, the deformation effect of small particles are slight, particles are presumed spherical and the diameter is constant [70]. Therefore constant diameter value is assigned for RBCs in this study, although RBCs are highly deformable particles.

3.2 Numerical Discretization and CFD

There are many partial differential equations (PDE) to define the physics in the nature. CFD is actually a branch of fluid dynamics that makes use of numerical methods to solve PDEs related to fluid flows. CFD requires to analyze PDEs with numerical methods to solve in linear equation Figure 3.3.

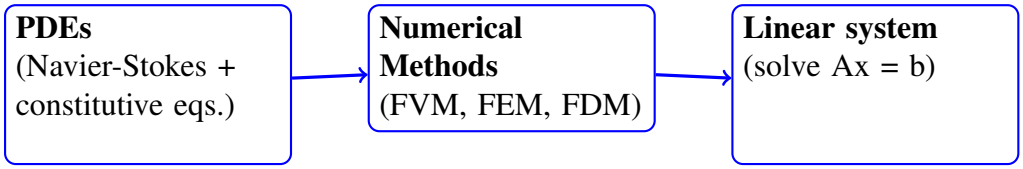

Figure 3.3 : Illustration of the CFD process

Finite Volume Method (FVM) in which governing equations such as continuity and momentum equations are used in the integral form, is used in this study. The computational mesh elements provide the discrete control volumes in which integrals of the governing equations are performed to obtain the numerical solution of the problem.

PDEs have generally a few analytical solutions due to their non-linear structure and are restricted to the simple geometries to get analytical solutions. Therefore it is needed to apply numerical methods to approximate to the solution of the flows which has no analytical solution. For that, PDEs are transformed in space and time to attain their counterparts. This process of transforming a PDE into its algebraic analogue

is termed numerical discretization. FVM is likely to be the most prevalent and far reaching approach for numerical discretization, especially for fluid dynamics. Utilizing FVM, the computational space is first partitioned into various nonoverlapping control volumes. That means, each control volume encompasses the grid point where the flow variables are present, later computed and stored. The governing conservation equations are converted into integral form to utilize FVM. The generalised conservation equation for a variable ϕ is;

$$\frac{\partial}{\partial t}\int\int\int_{\forall}\rho\phi d\forall+\int\int\int_{\forall}\nabla(\rho u\phi)d\forall=\int\int\int_{\forall}\nabla(\Gamma\nabla\phi)d\forall+\int\int\int_{\forall}S_{\phi}d\forall \quad (3.15)$$

The above equation needs to be simplified using i.e Gauss' divergence theorem which converts volume integrals into surface integrals. Converting the integrals is shown below with an arbitrary vector, f;

$$\int\int\int_{\forall}\nabla f d\forall=\int\int_{S}f.\mathbf{n}dS \quad (3.16)$$

where **n** is the unit vector.

Using Gauss' divergence theorem, the divergence term in the volume integrals of the partial differential equation are converted to surface integrals, which works for spatial discretization. With the divergence theorem, equation 3.15 becomes;

$$\frac{\partial}{\partial t}\int\int\int_{\forall}\rho\phi d\forall+\int\int_{S}\mathbf{n}.(\rho u\phi)dS=\int\int_{S}\mathbf{n}.(\Gamma\nabla\phi)dS+\int\int\int_{\forall}S_{\phi}d\forall \quad (3.17)$$

In OpenFOAM, all numerical schemes to discretize the flow equations are described in fvSchemes file and the discretized parameters varies due to the implemented model. For instance, with a turbulence model, additional parameters must be defined since the whole equation changes.

3.3 Boundary Conditions

There are two main types of boundary conditions which are used in CFD simulations such as Dirichlet and Neumann boundary conditions. Dirichlet boundary conditions are specified as values at boundary and Neumann boundary conditions contain derivatives at the boundary which is specified due to normal values.

In order to impose them on an ordinary or partial differential equation, it assigns the values that the solutions needs to hold on the boundary. On the other hand imposing Neumann BCs on an ODE or PDE, the derivative of a soluton is hold on the boundary.

Therefore, Dirichlet boundary conditions determine the value of a field on a boundary segment. Some physical examples are specifying the temperature on a surface that is in contact with a heat bath, or specifying that a viscous fluid "sticks" to a surface. In mathematical sense, dirichlet boundary can be defined in time-dependent 3D flow domain as,

$$f(x,y,z,t) = T \tag{3.18}$$

where Neuman boundary condition can be stated as,

$$f(x,y,z,t) = \frac{\partial T}{\partial n} = \hat{n} \bigtriangledown T \tag{3.19}$$

In OpenFOAM, these boundary conditions are defined as its own defined names such as fixedValue for Dirichlet, zeroGradient for Neuman boundary conditions. Both boundary conditions are used in the simulations such as Drichlet for inlet and Neumann for outlet boundary condition.

4. NUMERICAL MODELS

For the CFD simulations we used OpenFOAM the open source software in order to solve equations explained above with the proper initial and boundary conditions. Specifically, the modified Carreau-Yashauda model is coded inside OpenFOAM. All other physics models such as drag and lift force model, two-phase modelling and etc. were in functionality of OpenFOAM. As multiphase modelling we used Mixture Theory which means Eulerian-Eulerian model. All residuals are set to 1e-7 for as convergence criteria.

4.1 Benchmark Models

Since complex hemodynamics of the blood flow is approximated with numerical models, CFD models in this regards should be validated by comparing the CFD results with the experimental data. For the validation of proposed numerical model, two different flow domians such as a micro-channel geometry and an expansion channel geometry are tested to validate our numerical methods with the existing experimental data.

4.1.1 Micro-channel model

The bottom boundary from which the fluid is supposed to enter the model is the velocity inlet of the model and the top boundary from which the blood supposed to leave the domain is the outlet of the model where the rest of the boundaries are defined as no-slip wall boundary condition in the simulations.

The geometry of micro channel is referenced from the study of Wu et al. [52] and the grid are shown in Figure 4.1. The channel has 100 μm depth in z direction. The mesh of the micro-channel geometry is created using blockMesh module of OpenFOAM as structured grid in which the elements near walls are finer.

Initial and boundary conditions used are in micro-channel model [52] are shown in Table 4.1 and the boundary conditions in Table 4.2.

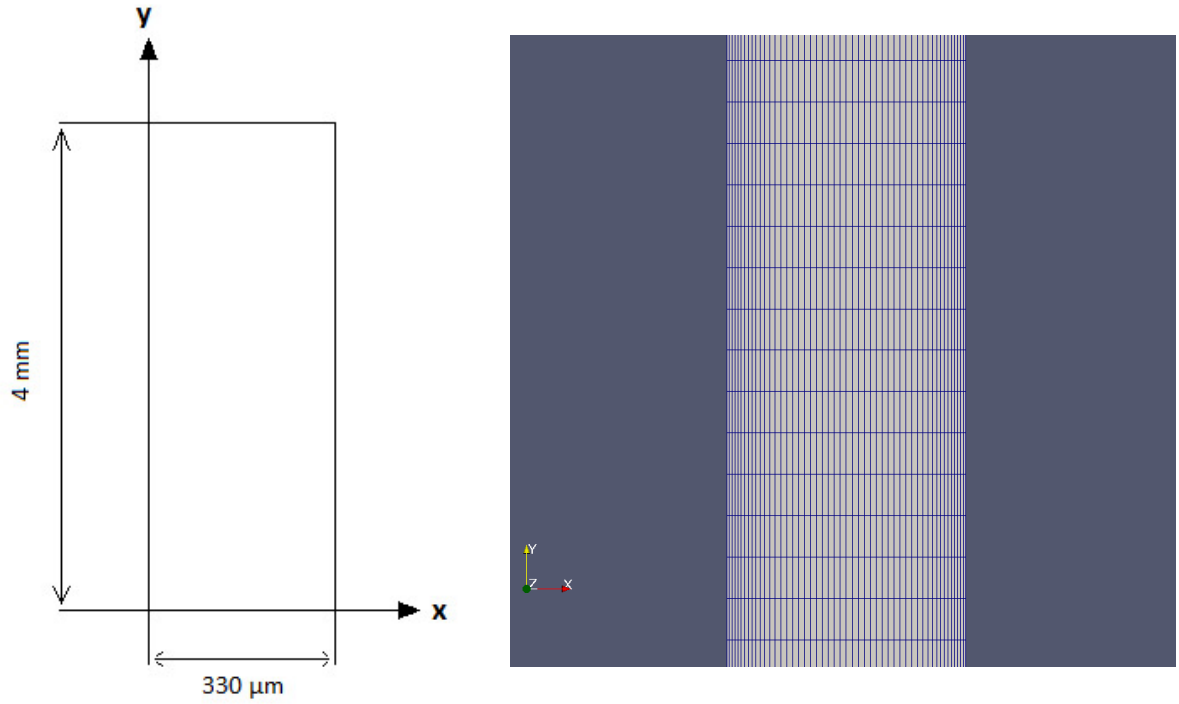

Figure 4.1 : The sizes and the mesh structure of the micro-channel model.

Table 4.1 : Initial conditions and blood parameters

Initial Conditions	Values
Inlet velocity	350 $\mu m/s$
Hematocrit	%45
Plasma density ρ_{plasma}	1027 kg/m^3
RBCs density	1100 kg/m^3
Plasma viscosity	0.00096 $Pa.s$

Table 4.2 : Boundary conditions of micro-channel model

Boundary	Inlet	Outlet	Walls
Velocity	fixedValue	zeroGradient	noSlip
Pressure	zeroGradient	prghPressure	zeroGradient
Volume Fraction	fixedValue	zeroGradient	zeroGradient

This model is created for the validation of our numerical model with experimental data published by Patrick et al [71].

The simulation of the micro channel model has been run in 20 seconds physical time to get the steady-state channel flow solution of blood.

The velocity profile of RBCs as a function of x at y=2.5 mm, and depth z=16 μm and z=8 μm is shown in Figure 4.2,

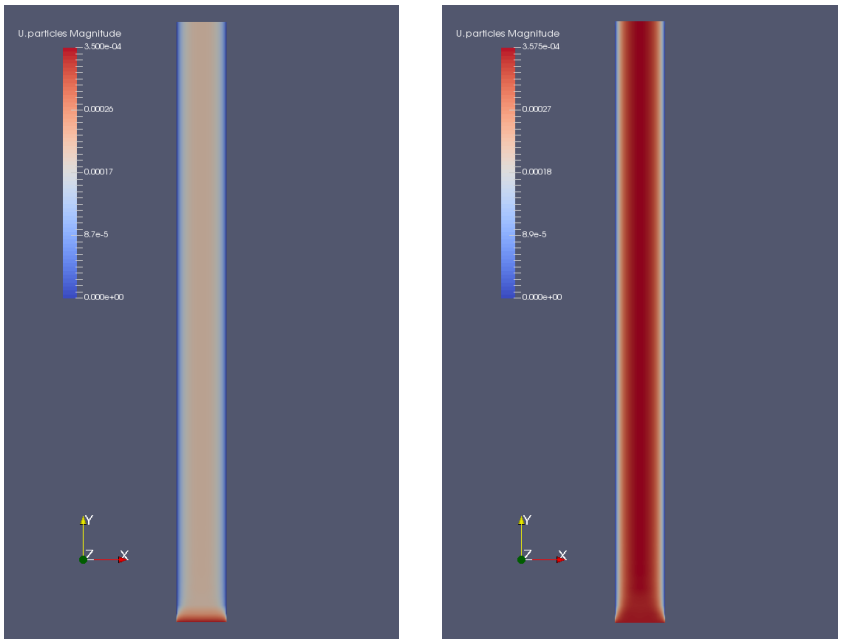

Figure 4.2 : Velocity contours of RBCs in the micro channel model for the cross section of $8\mu m$ and $16\mu m$, respectively.

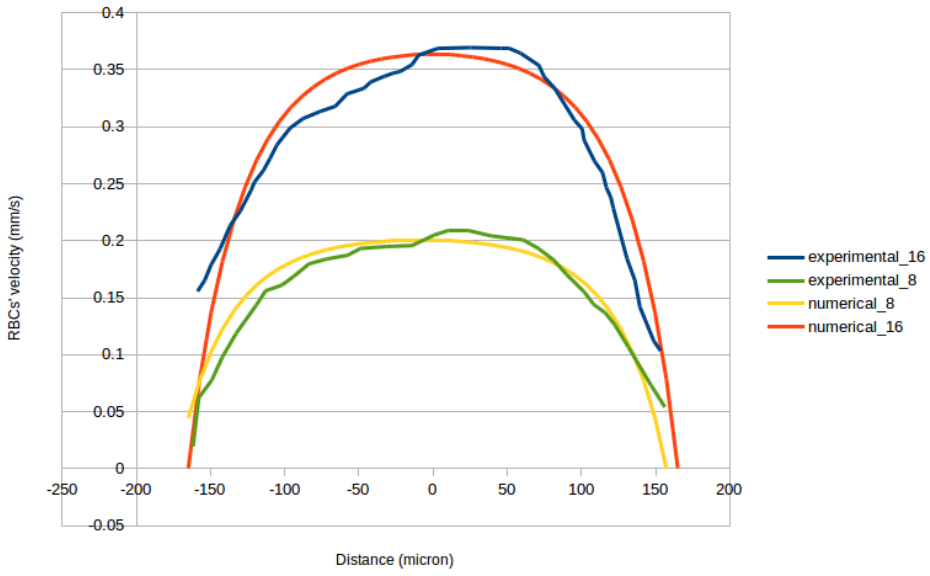

Figure 4.3 : The velocity profile of RBCs as a function of x on the sample line at y=2.5 mm, and depth z=16 μm, z=8 μm with the experimental data.

Obtained numerical results agree considerably with the experimental data which is shown in Figure 4.3. Therefore, our numerical model is suitable for low shear rates.

4.1.2 Axisymmetric expansion channel model

Tubular sudden expansion channel geometry is constructed axisymmetric and the mesh is created accordingly. Major dimensions of the geometry is given in Figure 4.4

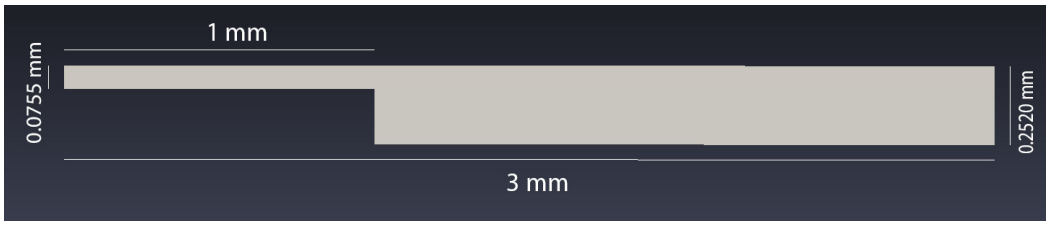

Figure 4.4 : Sizes of the expansion channel model

The same boundary conditions are applied for this domain together with axisymmetric side planes which is called "wedge" in OpenFOAM. The mesh of sudden expansion channel geometry is directly created using OpenFOAM as axisymmetric. In this case, Reynolds number dependent two cases such as Re=12.2 and Re=3.8 are presented due to the experimental data [72] which provides the data of the velocity on the line through the center of the vortex. Therefore the velocity values are extracted from the sample line of the numerical results in order to compare with the experimental data [72]. Also, attachment points for both cases are shown in Figure 4.5,4.6. The numerical results show considerably good agreement with the experimental data.

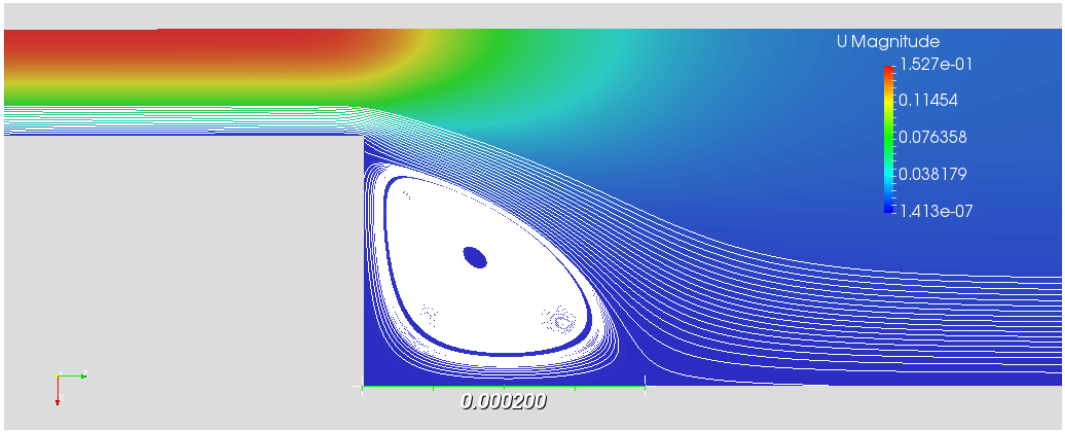

Figure 4.5 : Velocity contours of the numerical results for Re =12.2 with 1% hardened human red cells (d_p = 7.5 μm, ρ = 1.13 g/cm^3) dispersed in water (ρ = 1.0 g/cm^3 , μ = 0.01 P).

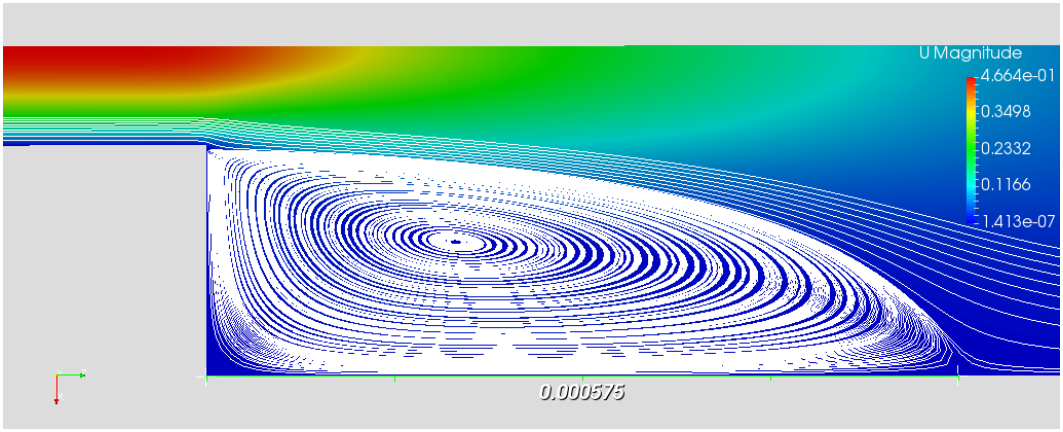

Figure 4.6 : Velocity contours of the numerical results for Re =37.8 with 1% hardened human red cells (d_p = 7.5 μm, ρ = 1.13 g/cm^3) dispersed in water (ρ = 1.0 g/cm^3 , μ = 0.01 P).

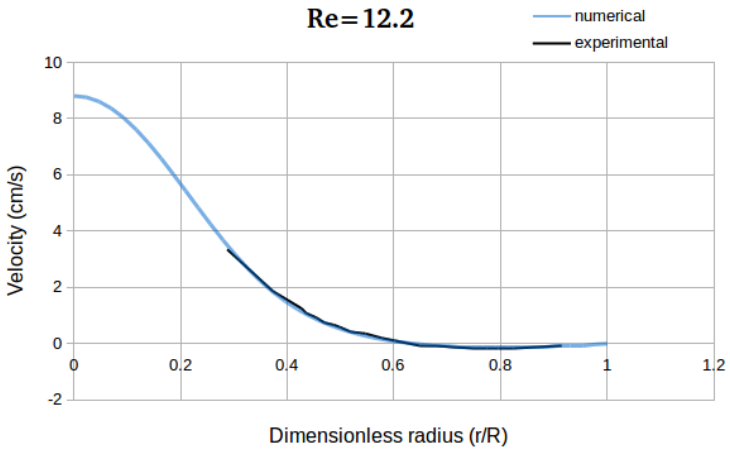

(a) Re = 12.2 and U_{inlet} = 75.7 mm/s

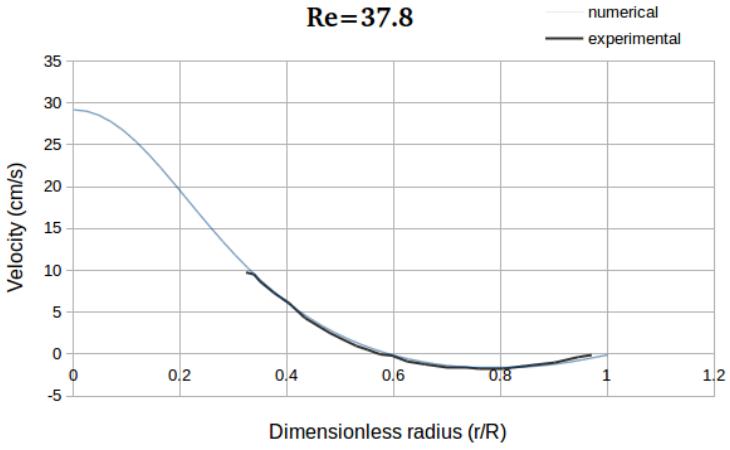

(b) Re = 37.8 and U_{inlet} = 233 mm/s

Figure 4.7 : Numerical results in comparison with the experimental data [72] for 1% hardened human red cells (d_p = 7.5 μm, ρ = 1.13 g/cm^3) dispersed in water (ρ = 1.0 g/cm^3 , μ = 0.01 P).

The sudden expansion model has the experimental data for %99 water and %1 hardened human red cells. In order to see the single phase model and two-phase model even there is a small percentage of red cells, single phase water flow simulation is also conducted in the same geometry. The result of the single phase simulation does not show the good agreement with the experimental data.

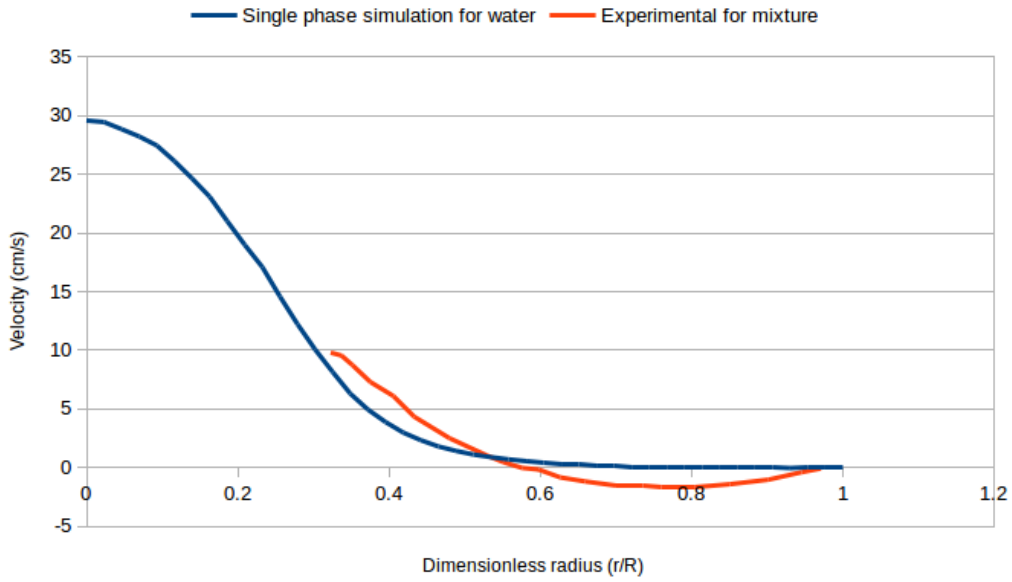

Figure 4.8 : Single phase water flow and the experimental data comparison.

4.1.3 Deep Vein Model with Venous Valve

Three cases with a different positioning of the valves are analyzed for two-phase blood flow. A finer mesh is used in the region of venous valve to focus on the critical region next to the valves where blood flow is stagnant leading to potential clot formation. Figure 4.9 shows symmetry plane and close up view of deep vein model representing the patient actual deep vein. The geometries for DVT cases are referenced from a thesis [73] in the literature..

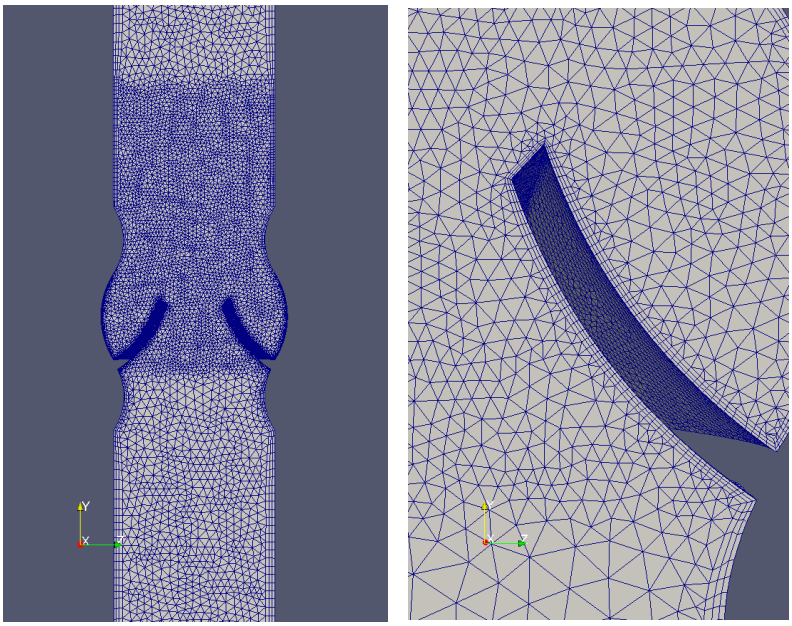

(a) Symmetry plane. (b) Close up view.

Figure 4.9 : The mesh and geometry of the vein model with venous valves (geometry 1)

Three different parietal valve positioning (short, wide, span) in deep vein model are studied (see in Figure 4.9, 4.10).

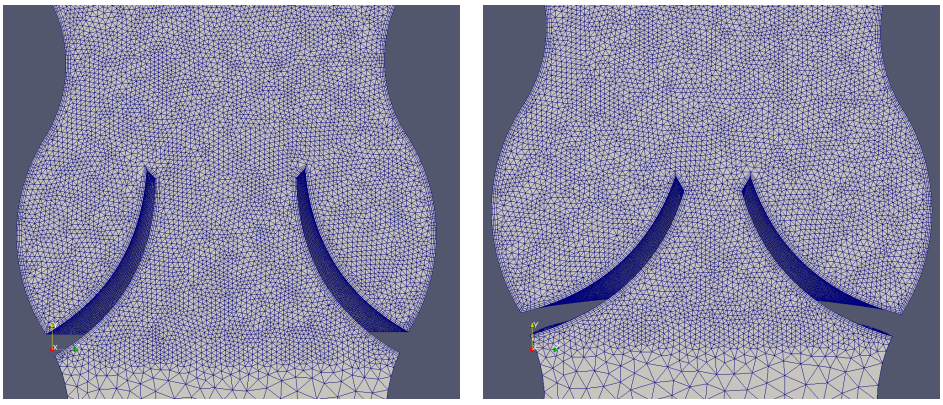

(a) Wide open valve. (b) Short open valve

Figure 4.10 : Valve openings of two different vein models with venous valves (geometry 2-3).

The quality of mesh can be checked in Icem CFD. The mesh quality was allright for convergence in CFD simulations using OpenFOAM. Additionally, $fluentMeshToFoam$ function is used to convert exported Fluent mesh from Icem CFD to OpenFOAM mesh. After that it is recommended to use *renumberMesh* function to renumber the elements of the mesh to decrease bandwith. This function put to use Cuthill-McKee algorithm, see [74] for the algorithm's detail.

5. RESULTS AND DISCUSSIONS

For the models to examine DVT, the inlet velocity of the blood is relatively higher than the validation cases which is 0.2 m/s. Although blood flows faster, there are statis points near the parietal valve. Therefore, modified Carreu-Yashuda model is important to investigate the flow near perietal valves. Implemented numerical model is suitable for low shear rates and able to track the regions where RBCs become probably denser which would lead possible clot forming.

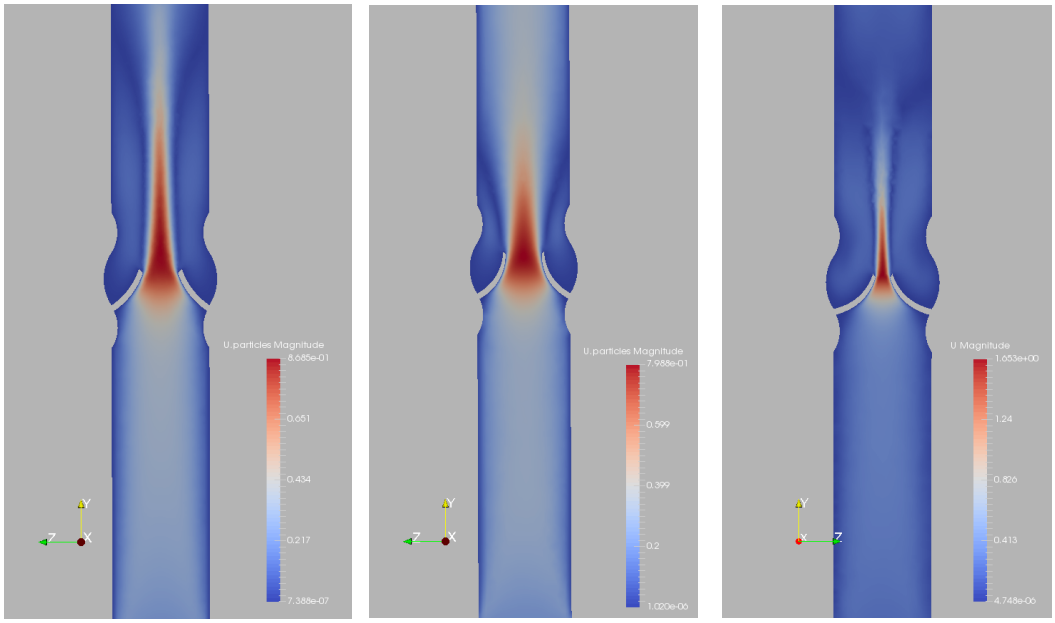

(a) Small valve model (b) Wide-open model (c) Short-span model

Figure 5.1 : RBCs' velocity profiles (m/s) at 1s.

In this study, RBC aggregation is important observe. RBCs aggregation is shown in Figure 5.2 as higher volume fraction than hematocrit%45.

In this thesis, RBCs aggregation is pointed out as the increase in the volume fraction of RBCs. Also, this aggregation is shown due to the different time stamps in Figure 5.7 for the wide-open valve model.

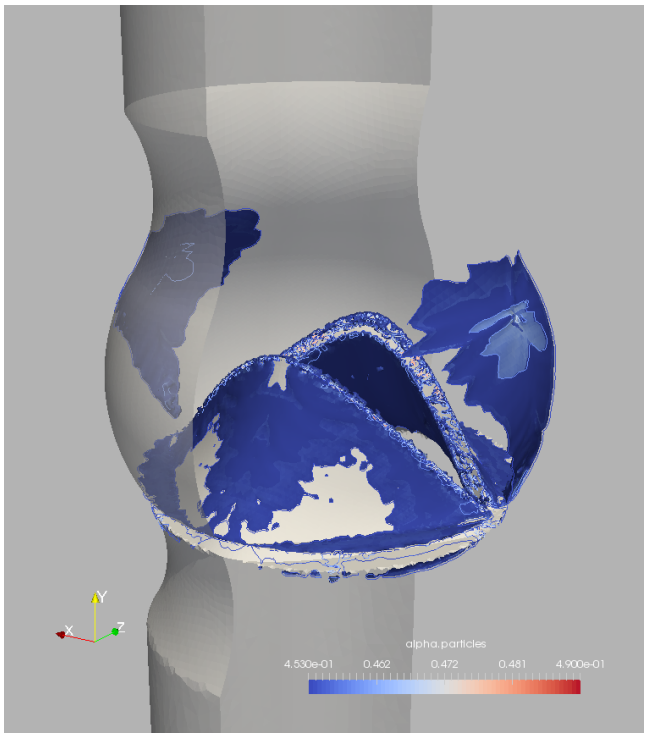

(a) Small valve model

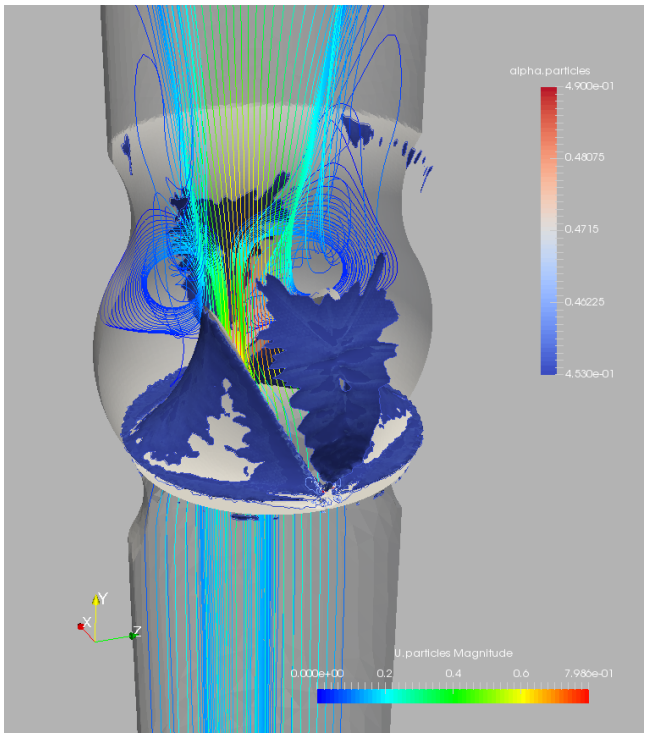

(b) Wide-open model

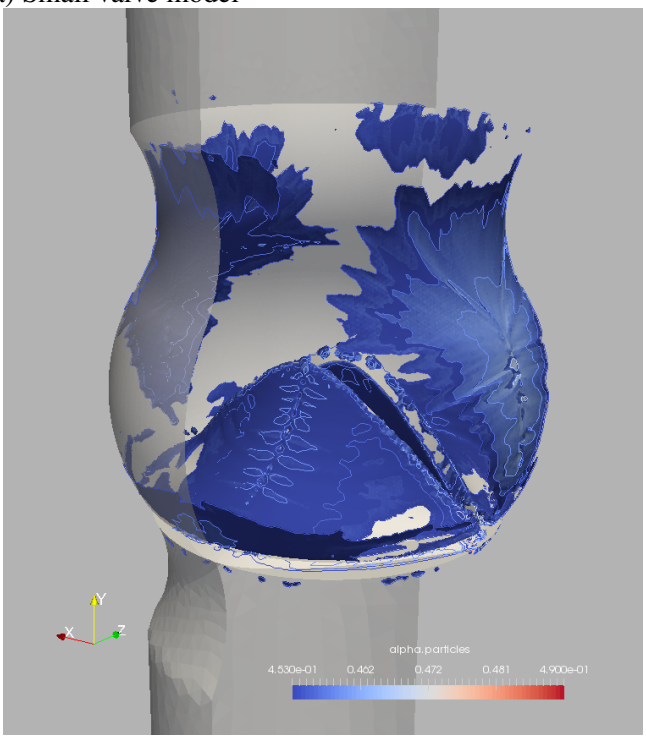

(c) Short-span model

Figure 5.2 : RBCs aggregation at 1s.

As it is seen in figures, the increase in the volume fraction of RBCs accumulates in time. The region behind valve is critical in terms of clot formation due to RBCs aggregation because of low shear rates. Additionally, reverse flow is observed in the region behind valve which would possibly contribute to RBCs aggregation, Figure 5.4.

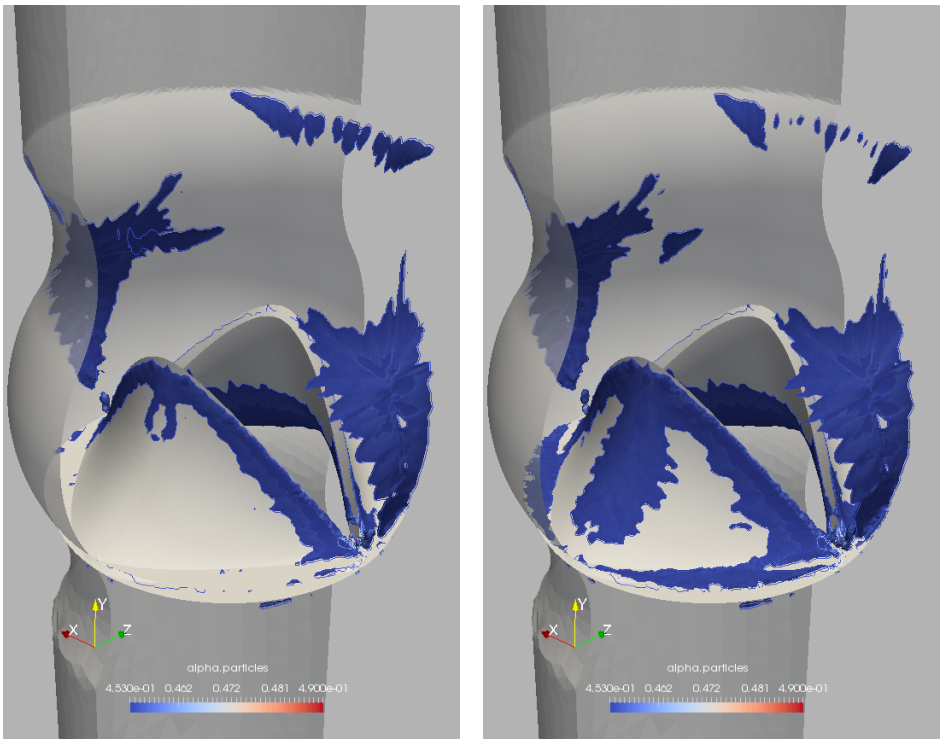

(a) at 0.5s (b) at 0.75s

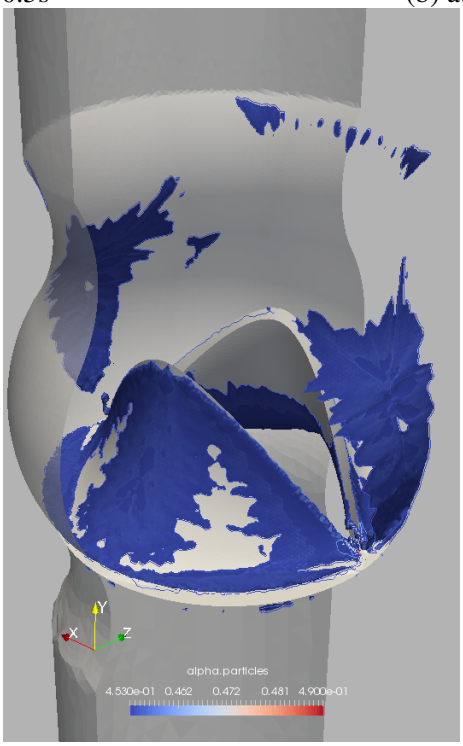

(c) at 1s

Figure 5.3 : RBCs aggregation due to different time stamps.

The results have been plotted on the sample lines through z direction at the points (a to e) shown in Figure 5.5. Samples from these points are extracted from all three DVT models. The sample lines from the beginning of the perietal valve to further are placed to observe velocity profiles and the volume fraction of RBCs, shear rate.

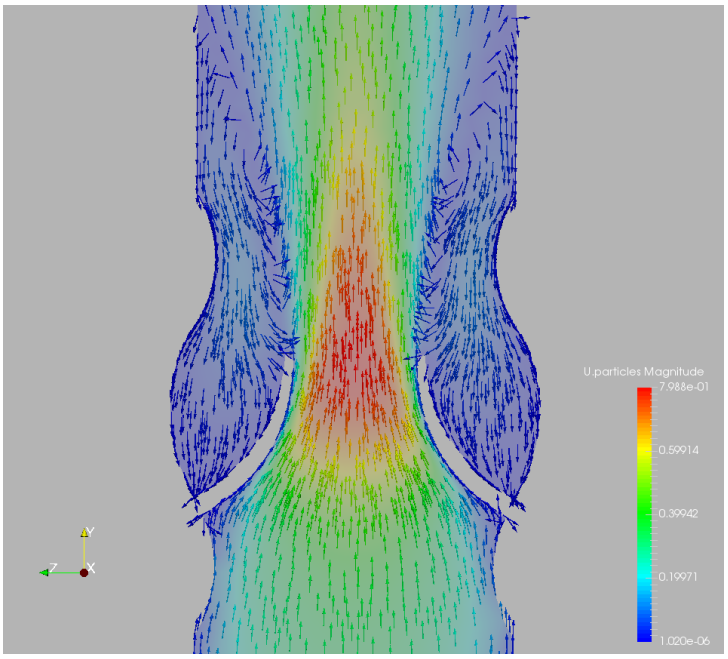

Figure 5.4 : Velocity vectors at 1s for the second model.

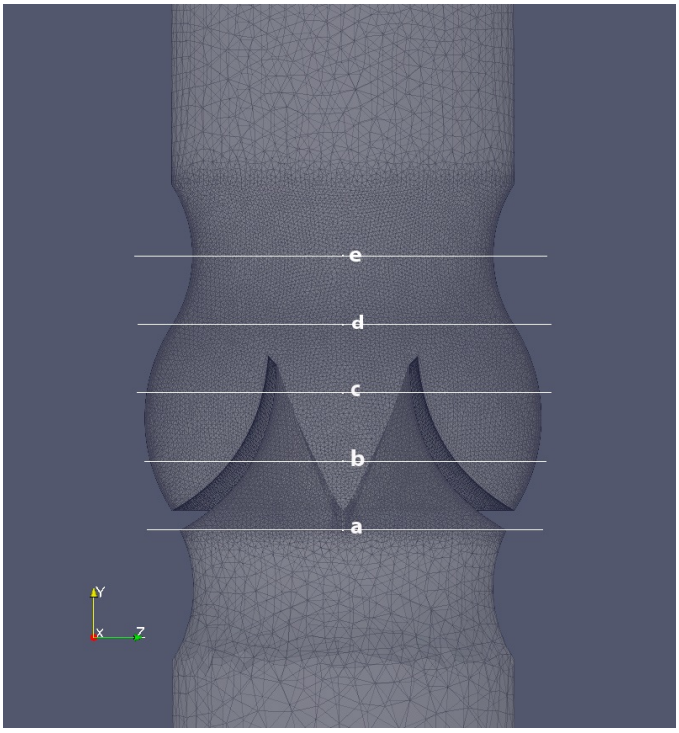

Figure 5.5 : Cross lines to observe flow parameters.

In two-phase blood flow model, plasma phase is considered as Newtonian flow and RBC phase Non-Newtonian where the shear thinning and viscoelastic behaviour is most observed. In RBC phase, the blood viscosity is modelled with modified Carreu-Yashuda approximation. Our main motivation is to observe potential RBC aggregation near the parietal valves and also to find the flow conditions leading to

statis condition and critical wall shear stress values. It is known that statis condition of blood may lead to a potential formation of clot or thrombosis. RBC aggregations are tracked by volume fractions flow parameters are observed by five cross lines shown in Figure 5.5. The velocity magnitudes and volume fractions are plotted through cross section of each line.

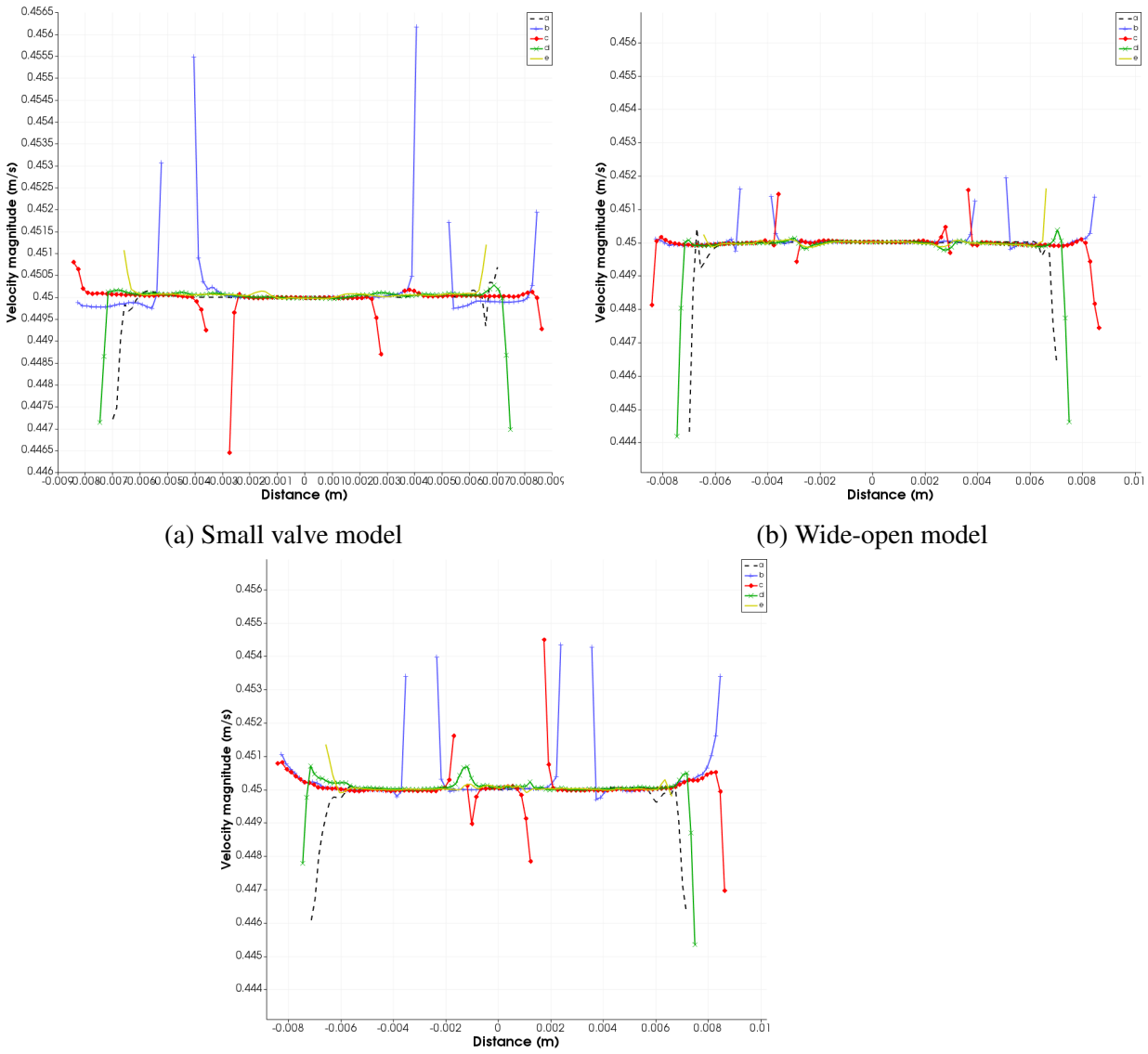

(a) Small valve model

(b) Wide-open model

(c) Short-span model

Figure 5.6 : RBCs' volume fractions on the sample lines.

It is observed that, RBCs aggregation slightly increased around lower sections of the valves and decreased at the tip of the valve. When the valve angle gets narrowed, the RBCs aggregation tends to increase at the lower sections of valve and decrease at the tip of the valve. It can be concluded that, with the increase of valve angle, this differences gets small.

In order to compare these models, the velocity profiles have also been plotted. Velocity gets narrowed and increases naturally with the short opening and thus the maximum velocity is observed in short-span model.

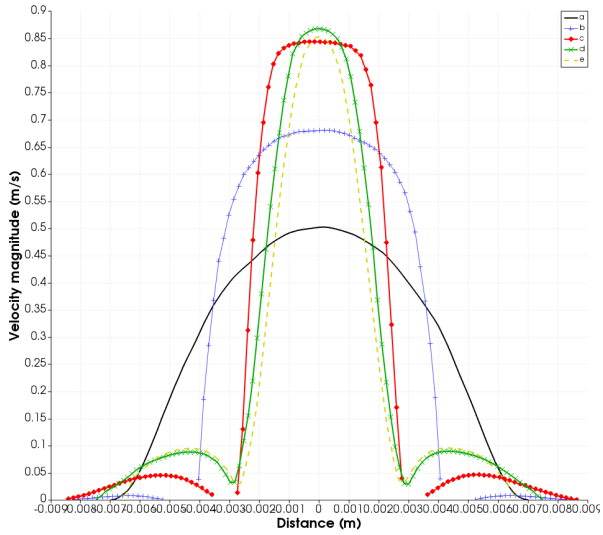

(a) Small valve model

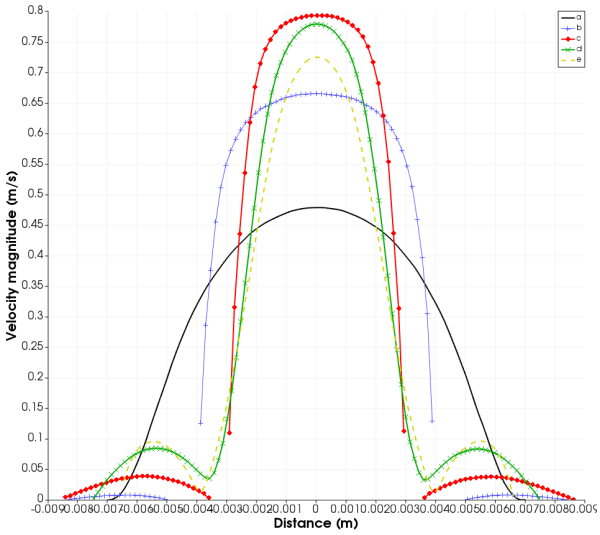

(b) Wide-open model

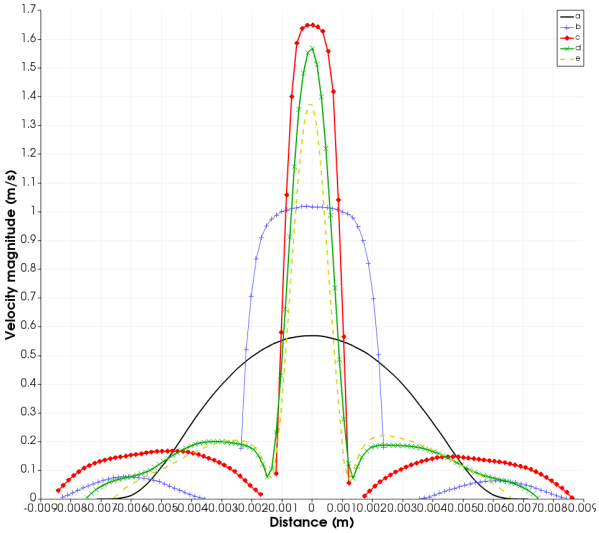

(c) Short-span model

Figure 5.7 : Velocity profiles of RBCs on the sample lines.

Small velocities shown in plots represent the field behind valve. As it is shown in Figure 5.4 reverse flow is present behind valve and the plots displays the magnitude of the reverse flow.

Since shear rates is a dependency of the viscosity of RBCs, their values are also observed near valve region. As expected, low shear rates are observed behind valve where is the critical region for clot formation.

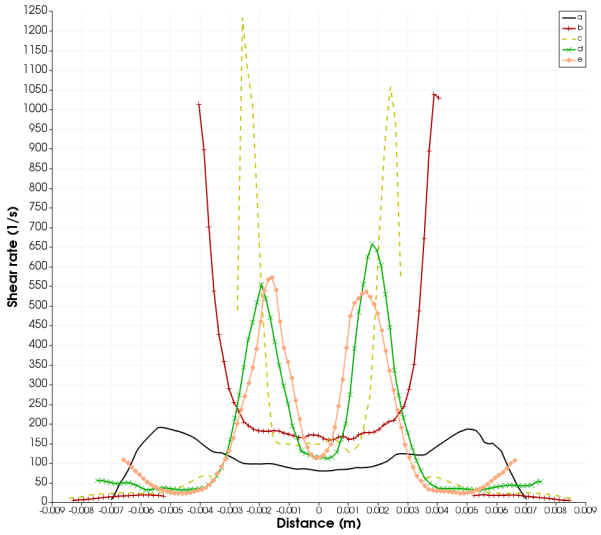

(a) Small valve model

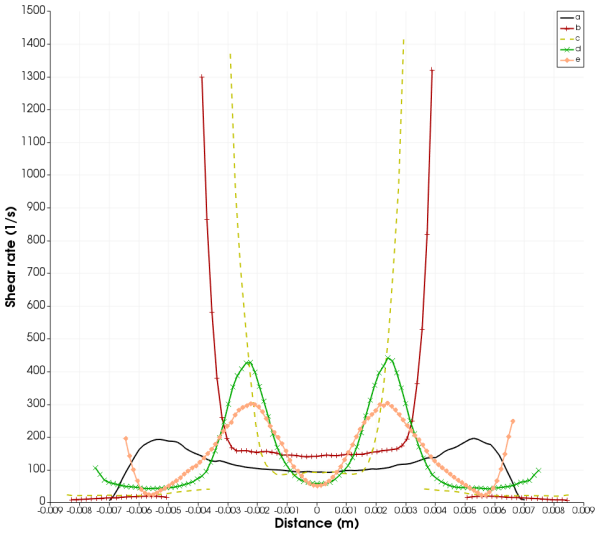

(b) Wide-open model

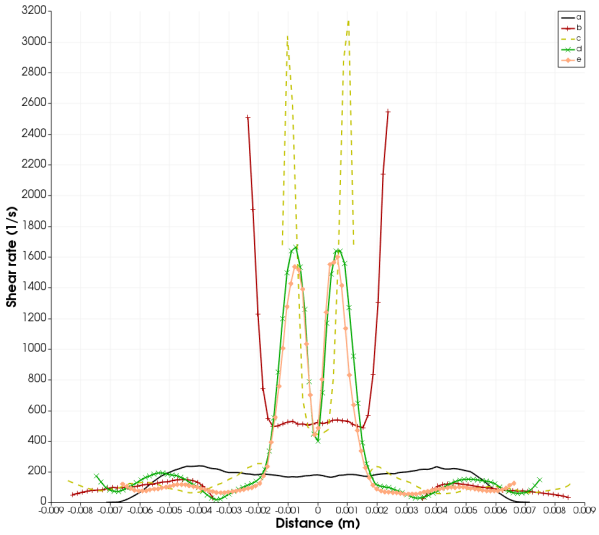

(c) Short-span model

Figure 5.8 : Shear rates of RBCs on the sample lines.

Due to the shear rates profile it can be said that the viscosity of RBCs increases behind the valve. Additionally, when the valve angle gets narrowed, shear rate at the same cross lines b and c, tend to increase higher. Cross lines of b and c show that shear rates increase drastically, especially inner surface of the valve. Additionally, 3D contours of shear rates of RBCs illustrates the critical regions well.

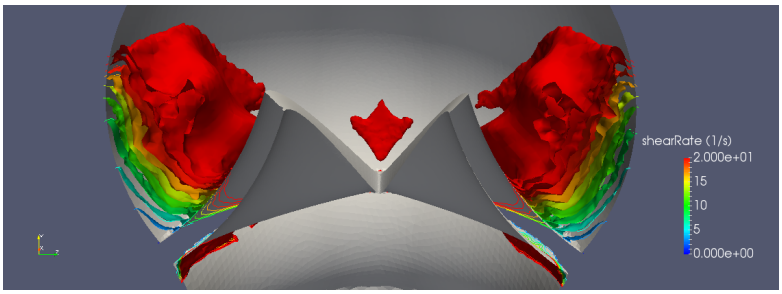

(a) Small valve model

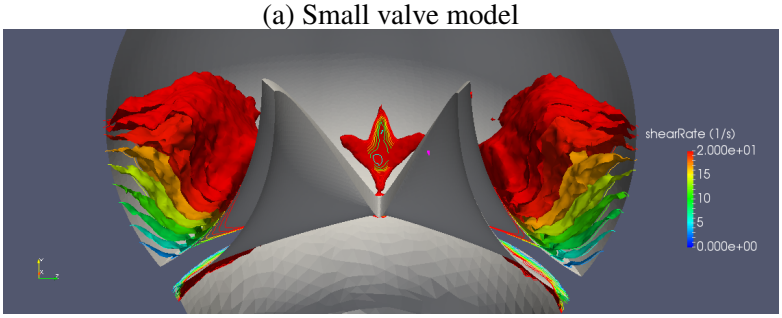

(b) Wide-open model

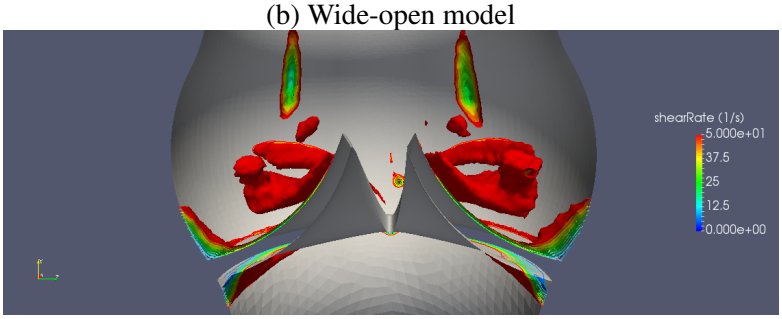

(c) Short-span model

Figure 5.9 : Shear rate contours of RBCs near valve.

5.1 Index Values

Our model is critical for the estimation of the formation of thrombosis in deep veins. Statis conditions has to be satisfied for the formation of thrombosis (blood clot). In order to understand how stasis conditions occur, we have to examine the variations of shear stress in blood. In the literature, there is currently no any evidence based index values. This study propose evidence based (shear stress) index value to numerically estimate the potential stasis condition and thus thrombus formation for the specific patient. The best shear stress based index value is Spatial Wall Shear Stress Gradient (SWSSG). Therefore WSS and SWSSG values of the numerical results have been studied as well.

5.1.1 Wall Shear Stress

Since the simulations are conducted as two-phase flow, WSS had to be calculated with the effect of both phases. Two important parameters to calculate WSS such as kinematic viscosity and derivation of the velocity gradient are obtained considering mixture fluid. Although high WSS cause trouble in veins for several cases, we look for the regions where WSS is small in order to observe stagnant regions. WSS contours for all three models are shown in Figure 5.10. The magnitudes of WSS in the contours represent incompressible values and thus the values are shown relatively smallar than usual WSS magnitudes.

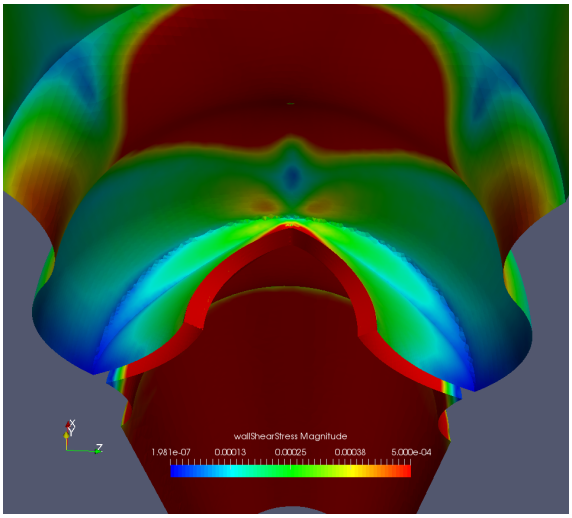

(a) Small valve model

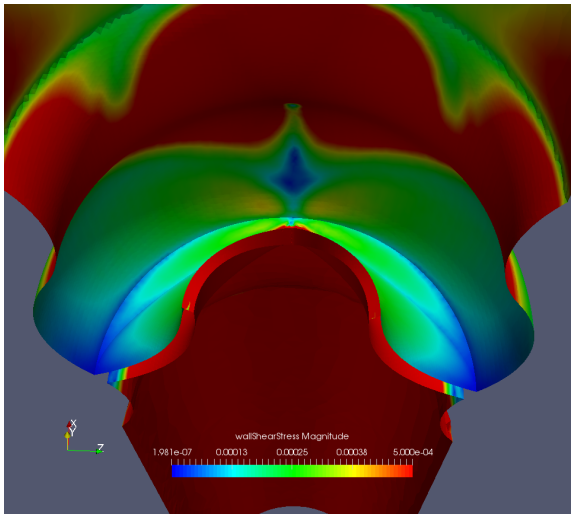

(b) Wide-open model

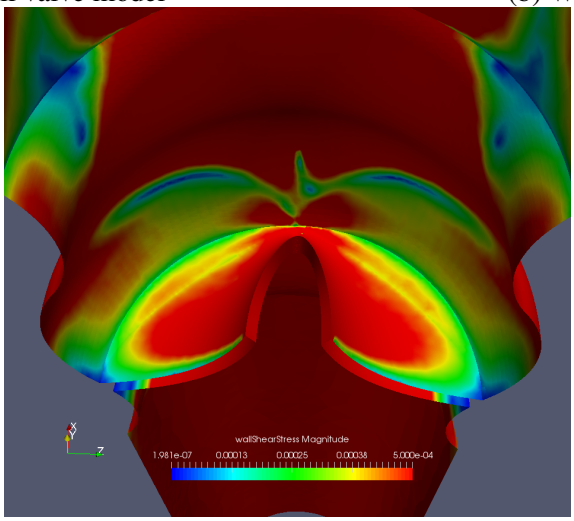

(c) Short-span model

Figure 5.10 : Wall Shear Stress Contours near valve.

5.1.2 Spatial Wall Shear Stress

SWSSG index values are calculated after obtaining WSS values. SWSSG is expressed in Equation 15.

$$SWSSG = \sqrt{(|\frac{\partial \overrightarrow{\tau_w}}{\partial x}|) + (|\frac{\partial \overrightarrow{\tau_w}}{\partial y}|) + (|\frac{\partial \overrightarrow{\tau_w}}{\partial z}|)} \tag{5.1}$$

As it is seen in the equation, this index value dictates the magnitude of the diagonal elements of the gradient of WSS. SWSSG and WSS together can show that the regions which have small SWSSG and WSS are highly stagnant.

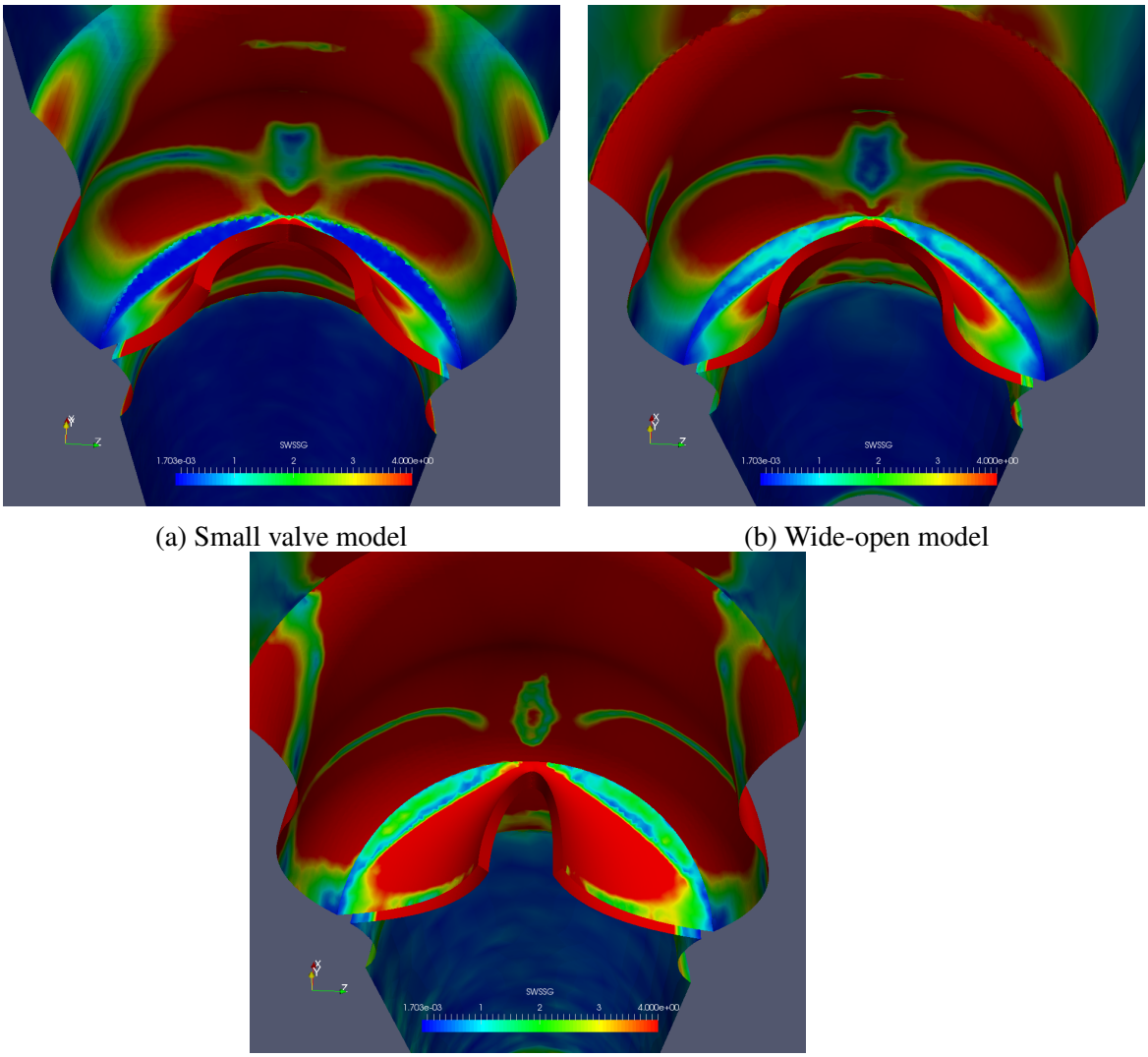

(a) Small valve model

(b) Wide-open model

(c) Short-span model

Figure 5.11 : Spatial Wall Shear Stress Gradient Contours near valve.

The conditions in blood such as stagnant regions and stasis points which cause clot formation, are the purpose of this thesis to examine. All results point out that the region behind valve is highly critical for RBCs aggregation. The region behind the valve with low shear rates, the presence of reverse flow, small WSS and SWSSG values on walls behind the valve shows the critical regions.

6. CONCLUSIONS

Computational Fluid Dynamics has become to play a significant role for investigating blood flow with the advancement and scalability in computational technology. Since there are many vein types in human body from large arteries to capillaries, hemodynamics of blood approximations vary due to the vein types as well as several parameters and condition. Therefore, modelling of blood flow is still challenging with its complex dynamics. On the other hand, circulatory system is crucial to understand the cardiovascular diseases in the body. For that, CFD can provide a different and efficient point of view to investigate blood flow. In this study, two-phase blood flow modelling in low shear rates is established to examine the blood flow in deep veins where venous valves are present. Even though blood flows not slowly in the vessel, it demonstrates stasis points near venous valve when the cusps are open due to its shape. Therefore modified non-Newtonian viscosity model for RBCs is significant to observe realistic hemodynamics.

It has been observed that due the opening of the venous valve, velocity profile changes significantly as well as WSS. As the opening of the venous valve increases, velocity of blood flow decreases and high WSS is seen on the edge of the cusps and where the cusps are joined together. Although high WSS which jeopardizes vein walls, is important to look for in blood flow, small WSS is more importantly examined because the aim is to observe stagnant regions near parietal valve. Moreover, reverse flow (vortices) is observed in those regions behind the cusps. The regions with low velocities where also reverse flow is present, are the possible clot formation regions. Due to the simulations, it can be seen that behind cusps, velocity is also very low and thus clot formation is more susceptible.

In addition to that, It can also be seen in the results that near those regions, the volume fraction of RBCs has increased during time. Our numerical model demonstrates straight increment of the volume fraction of RBCs behind cusps where the velocity

is low. The hematocrit which is 0.45 in the beginning, has increased 0.50 in some regions.

Furthermore, by using index values those critical regions can be tracked. Several index values can be applied to the patient blood and vein data and among those SWSSG has been obtained after the results. The index values to see stasis points, can also be interpreted as time-averaged. Therefore, the diagnosis of DVT using CFD would be more confidential by studying several index values. Only then, more realistic clot formation possibility in specific patient vein can be estimated.

As a condition of a flow, pressure drops from start to the end. In DVT models, there are huge pressure difference between the sides of the cusps. This pressure difference between cusps's side forces the valve to open and let blood flows through the valve which is illustrated in pressure contours. For more realistic and practical DVT cases this study demonstrates the necessity of Fluid Structure interaction (FSI) implementation in CFD simulations. FSI is actually necessary to reveal the health profile of patients with patient base simulations in deep veins because the effect of the wall movements are crucial as it disturbs RBCs aggregation.

6.1 Practical Application of This Study

In this study simulations has been conducted in vein representative geometries with venous valves. All geometries are designed in 3D CAD software by the author while referencing from the literature. However, the presented numerical model can be implemented to simulate blood flow in the vein geometries which is obtained by patients using MR images. Only then, possible cardiovascular diseases can be interpreted for that vein model and the patient. As it is mentioned before, FSI model should be implemented in the numerical model for the patient based vein geometry in order to see real circulation of blood related to the patient.

REFERENCES

[1] Heit JA, Melton LJ 3rd, Lohse CM, et al. "Incidence of venous thromboembolism in hospitalized patients vs community residents," Mayo Clin Proc. 2 0 01, 76 (11) :1102-1110.

[2] House of Commons Health Committee (2005) The prevention of venous thromboembolism in hospitalised patients. London: The Stationery Office.

[3] Rashid ST, Thursz MR, Razvi NA et al. (2005) Venous thromboprophylaxis in UK medical inpatients. Journal of the Royal Society of Medicine 98 (11): 507-12.

[4] White RH. The epidemiology of venous thromboembolism. Circulation. 2003;107(23 Suppl 1):I4-8.

[5] Janseen, Herbert. F, Jean Schachner, Joel Hubbard, and J. Ted Hartman. "The risk of deep venous thrombosis: A computerized epidemiologic approach." Surgery (Surgery), 1986: 205-212.

[6] Fowkes FJ, Price JF, Fowkes FG. Incidence of diagnosed deep vein thrombosis in the general population: systematic review. Eur J Vasc Endovasc Surg. 2003(1);25:1-5.]

[7] Anderson FA, Jr., Wheeler HB, Goldberg RJ, et al. A population- based perspective of the hospital incidence and case-fatality rates of deep vein thrombosis and pulmonary embolism. The Worcester DVT Study. Arch Intern Med. 1991;151(5):933-938.

[8] Dupin MM, et al. Modeling the flow of dense suspensions of deformable particles in three dimensions. Physical Review E. 2007;75(6):066707.

[9] Clausen JR, Reasor DA, Jr, Aidun CK. Parallel performance of a lattice-Boltzmann/finite element cellular blood flow solver on the IBM Blue Gene/P architecture. Computer Physics Communications. 2010;181(6):1013-1020.

[10] Zhang J, Johnson PC, Popel AS. Effects of erythrocyte deformability and aggregation on the cell free layer and apparent viscosity of microscopic blood flows. Microvascular research. 2009;77(3):265-272.

[11] Adkins J. Non-linear diffusion II. Constitutive equations for mixtures of isotropic fluids. Philosophical Transactions of the Royal Society of London. Series A, Mathematical and Physical Sciences. 1963;255(1064):635-648.

[12] Adkins JE. Non-linear diffusion i. diffusion and flow of mixtures of fluids. Philosophical Transactions of the Royal Society of London. Series A, Mathematical and Physical Sciences. 1963;255(1064):607-633.

[13] Shapir O, Lev M. The venous valve in the aged. Am Heart J. 1952;44:843-850.

[14] Bergan JJ, Schmid-Schönbein GW, Coleridge-Smith PD, Nicolaides AN, Boisseau MR, Eklof B. Chronic venous disease. N Engl J Med. 2006;355:488- 498.

[15] Lane RJ, Graiche JA, Cuzzilla ML, Coroneos JC. Incompetent venous valves: ultrasound imaging and exo-stent repair. Phlebolymphology. 2007;14:105-111.

[16] Aquila, A. "Deep Venous Thrombosis." Journal of Cardiovascular Nursing, July 2001 - Volume 15 - Issue 4 - pp 25-44

[17] Bergqvist D, Lowe G(2002) Venous thromboembolism in patients undergoing laparoscopic and arthroscopic surgery and in leg casts. Arch Intern Med 162:2173-2176

[18] Clayton, V. (2010, July 15). The Hidden Dangers of DVT. Retrieved from http://www.lifescript.com/health/centers/dvt/articles/the_hidden_dangers_of_dvt.aspx

[19] Virchow, R.L.K., Thrombose and Emolie. 1856, Frankfurt, Germany.

[20] NIH, Prevention of venous thrombosis and pulmonary embolism. Natl Inst Health Consens Dev Conf Consens Statement, 1986. 6(2): p. 1-8.

[21] Cotran, R.S., et al., Robbins pathologic basis of disease. 6th / ed. 1999, Philadelphia: Saunders. xv, 1425.

[22] Cho, Y. I. and K. R. Kensey, 1991, Effects of the non-Newtonian viscosity of blood on hemodynamics of diseased arterial flows: part 1, steady flows, Biorheology 28, 241-262.

[23] Steinman DA, Image-based computational fluid dynamics modeling in realistic arterial geometries. Ann Biomed Eng. 2002 Apr;30(4):483-97.

[24] Jung J, Hassanein A. Three-phase CFD analytical modeling of blood flow. Medical Engineering & Physics 30 (2008) 91-103.

[25] M. A. Xenos. An Euler-Lagrange approach for studying blood flow in an aneurysmal geometry. Proceedings of the Royal Society A Mathematical, Physical and Engineering Sciences. 10.1098/rspa.2016.0774.

[26] Valencia A, Ledermann D, Rivera R, Bravo E, Galvez M. Blood flow dynamics and fluid-structure interaction in patient-specific bifurcating cerebral aneurysms. International Journal for Numerical Methods in Fluids. 2008;58(10):1081-1100.

[27] Tomiyama Y, Brian JE Jr, Todd MM. Plasma viscosity and cerebral blood flow. Am J Physiol Heart Circ Physiol. 2000 Oct;279(4):H1949-54.

[28] Chien S, 1970. Shear dependence of effective cell volume as a determinant of blood viscosity, Science 168, 977-978

[29] Liu, IS. Continuum mechanics. Berlin: Springer-Verlag; 2002.

[30] Batra, Romesh C. Elements of continuum mechanics. Reston, VA: American Institute of Aeronautics and Astronautics (AIAA) Inc; 2006.

[31] Jung J, Lyczkowski RW, Panchal CB, Hassanein A. Multiphase hemodynamic simulation with pulsatile flow in a coronary artery. J Biomech 2006;39:2064-73.

[32] Van der Hoef M, et al. Multiscale modeling of gas-fluidized beds. Advances in Chemical Engineering. 2006; 31:65-149.

[33] Rajagopal, K.; Tao, L. Mechanics of Mixtures, Series on Advances in Mathematics for Applied Sciences, vol. 35. Singapore: World Scientific; 1995.

[34] Rusche, H. PhD Thesis. Imperial College; 2002. Computational fluid dynamics of dispersed two-phase flows at high phase fractions.

[35] H. G. Weller, G. Tabor, H. Jasak, C. Fureby, A tensorial approach to computational continuum mechanics using object-oriented techniques, COMPUTERS IN PHYSICS, VOL. 12, NO. 6, NOV/DEC 1998.

[36] Kim, J. PhD Thesis. Carnegie Mellon University; 2012. Multiphase CFD analysis and shape optimization of blood-contacting medical devices.

[37] G. de Simone, R. B. Devereux, S. Chien, M. H. Alderman, S. A. Atlas, J H Laragh. Relation of blood viscosity to demographic and physiologic variables and to cardiovascular risk factors in apparently normal adults. Circulation. 1990;81:107-117.

[38] Stoltz, J.F. et al.: Experimental approach to rouleau formation. Comparison of three methods. Biorheology Suppl. 1: 221-6 (1984)

[39] Ulker P., Sati L., Celik-Ozenci C., Meiselman H.J., "Mechanical Stimulation Of Nitric Oxide Synthesizing Mechanisms In Erythrocytes", BIORHEOLOGY, vol.46, pp.121-132, 2009.

[40] Mchedlishvili G., Maeda N., "Blood Flow Structure Related to Red Cell Flow: A Determinant of Blood Fluidity in Narrow Microvessels", Japanese Journal of Physiology, 51, 19-30, 2001.

[41] Popel AS, Johnson PC. Microcirculation and hemorheology. Annual Review of Fluid Mechanics. 2005;37:43-69.

[42] Maeda, N., 1996. Erythrocyte rheology in microcirculation. Jpn. J. Physiol. 46, 1-14.

[43] Baumler H, Neu B, Donath E, Kiesewetter H. Basic phenomena of red blood cell rouleaux formation biorheology. Biorheology. 1999;36:439-442.

[44] Stoltz J, Singh M, Riha P. Hemorheology in Practice. IOS Press; Amsterdam, Netherlands: 1999.

[45] Ben Ami R, Barshtein G, Zeltser D, Goldberg Y, Shapira I, Roth A, Keren G, Miller H, Prochorov V, Eldor A, et al., 2001. Parameters of red blood cell aggregation as correlates of the inflammatory state. Am J Physiol-Heart C. 280(5): H1982-H1988.

[46] Rampling MW, Meiselman HJ, Neu B, Baskurt OK. 2004. Influence of cell-specific factors on red blood cell aggrega- tion. Biorheology. 41(2):91-112.

[47] Kounov NB, Petrov VG. 1999. Determination of erythrocyte aggregation. Math Biosci. 157(1-2):345-356.

[48] Kim S, Popel AS, Intaglietta M, Johnson PC. 2006. Effect of erythrocyte aggregation at normal human levels on functional capillary density in rat spinotrapezius muscle. Am J Physiol-Heart C. 290(3):H941-H947.

[49] Anand M, Rajagopal K, Rajagopal KR. A model for the formation and lysis of blood clots. Pathophysiology of Haemostasis and Thrombosis. 2005; 34:109-120. [PubMed: 16432312]

[50] Yeleswarapu, KK. PhD Dissertation. University of Pittsbugh; 1994. Evaluation of continuum models for characterizing the con-stitutive behavior of blood.

[51] Brooks DE, Goodwin JW, Seaman GV. Interactions among erythrocytes under shear. Journal of Applied Physiology. 1970; 28(2):172-177. [PubMed: 5413303]

[52] Wu W, Aubry N, Massoudi M. Channel Flow of a Mixture of Granular Materials and a Fluid. ASME. ASME International Mechanical Engineering Congress and Exposition, Volume 7A: Fluids Engineering Systems and Technologies ():V07AT08A033. doi:10.1115/IMECE2013-65385.

[53] Van der Heiden K, Groenendijk BC, Hierck BP, Hogers B, Koerten HK, Mommaas AM, Gittenberger-de Groot AC, Poelmann RE (2006) Monocilia on chicken embryonic endocardium in low shear stress areas. Dev Dynam 235(1):19

[54] Topper JN, Gimbrone MA Jr. (1999) Blood flow and vascular gene expression: fluid shear stress as a modulator of endothelial phenotype. Mol Med Today 5(1):40-46

[55] Hierck BP, van der Heiden K, Poelma C, Westerweel J, Poelmann RE (2008) Fluid shear stress and inner curve remodeling of the embryonic heart. choosing the right lane! Sci World J

[56] McCormick SM, Eskin SG, McIntire LV, Teng CL, Lu CM, Russell CG, Chittur KK (2001) DNA microarray reveals changes in gene expression of shear stressed human umbilical vein endothelial cells. Proc Natl Acad Sci 98(16):8955

[57] Weinbaum S, Zhang X, Han Y, Vink H, Cowin SC (2003) Mechanotransduction and flow across the endothelial glycocalyx. Proc Natl Acad Sci 100(13):7988-7995

[58] Janmey PA, McCulloch CA (2007) Cell mechanics: integrating cell responses to mechanical stimuli. Annu Rev Biomed Eng 9:1-34

[59] Ku DN, Giddens DP, Zarins CK, Glagov S (1985) Pulsatile flow and atherosclerosis in the human carotid bifurcation. positive correlation between plaque location and low oscillating shear stress. Arterioscler Thromb Vasc Biol 5(3):293-302

[60] Soulis JV, Farmakis TM, Giannoglou GD, Hatzizisis YS, Giannakoulas GA, Parcharidis GE, et al. Molecular viscosity in the normal left coronary arterial tree. Is it related to atherosclerosis? Angiology. 2006; Vol 57, Issue 1, pp. 33-40.

[61] Meng H, Wang Z, Hoi Y, Gao L, Metaxa E, Swartz DD, Kolega J. Complex hemodynamics at the apex of an arterial bifurcation induces vascular remodeling resembling cerebral aneurysm initiation. Stroke. 2007;38:1924-1931.

[62] Meng H, Metaxa E, Gao L, Liaw N, Natarajan SK, Swartz DD, Siddiqui AH, Kolega J, Mocco J. Progressive aneurysm development following hemodynamic insult. J Neurosurg. 2011;114:1095-1103.

[63] Metaxa E, Tremmel M, Natarajan SK, Xiang J, Paluch RA, Mandelbaum M, Siddiqui AH, Kolega J, Mocco J, Meng H. Characterization of critical hemodynamics contributing to aneurysmal remodeling at the basilar terminus in a rabbit model. Stroke. 2010;41:1774-1782.

[64] Wang Z, Kolega J, Hoi Y, Gao L, Swartz DD, Levy EI, Mocco J, Meng H. Molecular alterations associated with aneurysmal remodeling are localized in the high hemodynamic stress region of a created carotid bifurcation. Neurosurgery. 2009;65:169-177. discussion 177-178.

[65] Schirmer CM, Malek AM. Computational fluid dynamic characterization of carotid bifurcation stenosis in patient-based geometries. Brain Behav. 2012;2:42-52.

[66] Schirmer CM, Malek AM. Wall shear stress gradient analysis within an idealized stenosis using non- Newtonian flow. Neurosurgery. 2007;61:853-863. discussion 863-864.

[67] Wojnarowski, J. (2001), Numerical study o f bileaf heart valves performance., in 'International Scientific Practical Conference: Efficiency o f Engineering Education in X X Century', Donetsk Ukraine.

[68] Schiller, L. and Naumann, A., 1933. A drag coefficient correlation, VDI Zeitschrift, 77, 318-320.

[69] Iimura K, Higashitani K. Simulation of the hydrodynamic drag force on aggregates. Adv Powder Technol 2005;16:87-96.

[70] Hadamard, 1911, Comptes rendus de l' académie des sciences V152, p1735.

[71] Patrick, M. J., C.-Y. Chen, D. H. Frakes, O. Dur, and K. Pekkan, 2011, Cellular-level near-wall unsteadiness of high-hematocrit erythrocyte flow using confocal PIV. Experiments in Fluids, 50(4):887-904.

[72] Karino T, Goldsmith HL. Flow Behaviour of blood cells and rigid spheres in an annular vortex. Philosophical Transactions of the Royal Society B 1977;279:413–45.

[73] Parimi, U. MSc Thesis. University of Texas at El Paso; 2010. Computational Fluid Dynamics Analysis of Deep Veins with Focus on Deep Vein Thrombosis.

[74] E. Cuthill and J. McKee. Reducing the bandwidth of sparse symmetric matrices In Proc. 24th Nat. Conf. ACM, pages 157–172, 1969.

APPENDICES

APPENDIX A.1 - Implementation details of the transport model in OpenFOAM

Simulations have been conducted by using OpenFOAM which is open source CFD software. Among many solvers of OpenFOAM, blood flow model is implemented in a developed solver based on twoPhaseEulerFoam. Two-phase incompressible fluid (solver is also capable of simulating compressible fluids) with one phase dispersed (RBCs) in continous phase (plasma) are simulated performing Eulerian-Eulerian mixture theory such that each phase is treated as a continuum. In order to define new viscosity model, a new transport model which is volume fraction and shear rate dependent is created in thermopysicalModel. Although energy equations are applied in twoPhaseEulerFoam, there is no specific boundary condition is applied related to temperature. Therefore the flow can be considered as isothermal.

In OpenFOAM, four transport models are prepared as in the source codes. Therefore new viscosity model which is mentioned in Section 2 is implemented.

E.g. thermophysical properties of the solid particles in mixture are given by,

```
thermoType
{
    type heRhoThermo;
    mixture pureMixture;
    transport const;
    thermo hConst;
    equationOfState rhoConst;
    specie specie;
    energy sensibleInternalEnergy;
}
```

Red line is what is changed to implement new viscosity model. Models available in OpenFOAM is shown below (see User Guide).

Table A.1 : Transport models in OpenFOAM

Transport properties	transport
constTransport	Constant transport properties
polynomialTransport	Polynomial based temperature-dependent transport properties
sutherlandTransport	Sutherland's formula for temperature-dependent transport properties

Copy the solver outside of the OpenFOAM folder (e.g. user directory)
cd $WM_PROJECT_USER_DIR/applications/solvers/bloodFoam
cp -r $WM_PROJECT_DIR/applications/solvers/bloodFoam
mv twoPhaseEulerFoam bloodFoam
cd bloodFoam
mv twoPhaseEulerFoam.C bloodFoam.C
Modify Make/files to;
bloodFoam.C

EXE = $(FOAM_USER_APPBIN)/bloodFoam
Clean and compile
wclean
wmake
After that, the same stages are done again to copy
"thermophysicalModels" library
Copy the "specie" folder in your user directory
cd $WM_PROJECT_USER_DIR /src/thermophysicalModels
cp -r $WM_PROJECT_DIR/src/thermophysicalModels/specie .
cd specie
Modify the Make/files to
LIB = $(FOAM_USER_LIBBIN)/libspecie
Clean and compile
wclean lib
wmake libso
Copy the "basic" folder in your user directory
cd $WM_PROJECT_USER_DIR /src/thermophysicalModels
cp -r $WM_PROJECT_DIR/src/thermophysicalModels/basic .
Modify the Make/files to
LIB = $(FOAM_USER_LIBBIN)/libfluidThermophysicalModels
Add the lines above in Make/options file
EXE_INC = \
-I $(WM_PROJECT_USER_DIR)/src/thermophysicalModels/specie/lnInclude
LIB_LIBS = \
-L$(FOAM_USER_LIBBIN)
Clean and compile
wclean libso
wmake libso

After that, new transport model is defined in user src/thermophysicalModels/specie/include/thermoPhysicsTypes.H by adding these lines,

```
typedef
bloodTransport
<
  species::thermo
  <
    hConstThermo
    <
      perfectGas<specie>
    >,
    sensibleEnthalpy
  >
> bloodGasHThermoPhysics;
```

Finally, new transport model folder is created in user src/thermophysicalModels/specie e.g. "constTransport" into "bloodTransport". The name of the files inside this transport

model also is changed into bloodTransport. In order to define new viscosity model inside this transport model mu() function is tracked by 'grep -nr "mu(" ' command via terminal.

```
thermoType
{
type heRhoThermo;
mixture pureMixture;
transport const;
thermo hConst;
equationOfState rhoConst;
specie specie;
energy sensibleInternalEnergy;
}
```

After compiling transport model with the new name without code modification, the thermophysical model which is shown below can be used in simulations, The mu() function is called in /src/thermophysicalModel/basic/rhoThermo/heRhoThermo.C file. heRhoThermo is blood's thermo type in which transport model of blood can be called including volume fraction and shear rate. Moreover mu() function resides in /src/thermophysicalModel/specie/transport/bloodTransport/bloodTransportI.H file as it is shown below;

```
template<class Thermo>
inline Foam::scalar Foam::bloodConstTransport<Thermo>::mu
(
const scalar p,
const scalar T
) const
{
   return mu_;
}
```

As it's seen, viscosity is directly assigned what is written in thermophysicalModel file which resides in /constant folder. Moreover mu() function passes two scalar values such as pressure and temperature. However they are not important in our case. We have to call the volume fraction and the shear rate. As it is mentioned before, mu() function is called in heRhoThermo.C file. This class can not access the volume fraction of RBCs e.g. alpha1. However alpha1 value can be call using objectRegistry class, thanks to the creative architecture of OpenFOAM. These lines are added into heRhoThermo.C file.

```
const volScalarField& alpha1 = this->db().objectRegistry
::lookupObject<volScalarField>("alpha.blood");
```

Thanks to objectRegistry::lookupObject<&type>() function we can access the volume fraction of the phase 1. "alpha.blood" is actually what user defines the name of thermophysical fluid in the beginning inside constant folder. For example in bubbleColumn tutorial it is "alpha.air" and "alpha.water".

After obtaining volume scalar field of the volume fraction, it can be passed into loop and mu() function to calculate new viscosity.

```
forAll(TCells, celli)
{
const typename MixtureType::thermoType& mixture_ =
this->cellMixture(celli);
TCells[celli] = mixture_.THE
(
hCells[celli],
pCells[celli],
TCells[celli]
);
psiCells[celli] = mixture_.psi(pCells[celli], TCells[celli]);
rhoCells[celli] = mixture_.rho(pCells[celli], TCells[celli]);
muCells[celli] = mixture_.mu(pCells[celli], TCells [celli], alpha1Cells[celli],
srCells[celli]); // alpha1 and shear rate are added to the function.
alphaCells[celli] = mixture_.alphah(pCells[celli], TCells[celli]);
}
```

As it is seen below, the function needed two parameters before modifying. Therefore mu() function needs to be modified in header files as well. Otherwise it will give an error.

Furthermore, author could not access neither the velocity(volVectorField) nor the tensor(volTensorField) of the phase 1 by using objectRegistry::lookupObject<&type>() function. Because of that the new vector field for velocity (volVectorField) is created inside heRhoThermo.C file such as,

```
const fvMesh& this->T_mesh();
tmp<volScalarField> sr //shear rate
(
new volScalarField
(
IOobject
(
"sr",
mesh.time().timeName(),
mesh,
IOobject::MUST_READ,
IOobject::NO_WRITE
),
mesh
)
);
const volScalarField& sr_ = sr.ref();
```

This means IOobject reads datas from a file named "sr" for everytime this class is in the action. This "sr" file contains the data of the magnitude of shear rate which

was mentioned in Chapter 3. In order to read the file, some modifications are made in the main source code(bloodFoam.C). After the program starts, inside time-loop, it calculates the strain rate then write into "sr" file in every timestep. When the algorithm goes to calculate viscosity of the new transport model in bloodFoam, the strain rate is read from recently saved "sr" file.

The modification in solver code is shown below,

```
const volScalarField sr_ = sqrt(2)*mag(symm(fvc::grad(U1)));
volScalarField sr
(
IOobject
(
"sr",
runTime.timeName(),
mesh,
IOobject::NO_READ,
IOobject::NO_WRITE
),
sr_
);
sr.write()
```

heRhoThermo class now can access the strain rate tensor field then calculate the custom viscosity.

There is also more efficient way to call strain rate inside thermoPhysicalModel library. Velocity magnitude can be called inside "correct" function as shown below. However, parameter TR must be defined in the definition code of "correct" as well in order to pass the value into "calculate" function. The real function to calculate the properties of the phase such as viscosity is actually "calculate" function. In this way, shear rate value is not necessarily written in harddisk in every timestep. However, constructor of heRhoThermo class also calls calculate in the beginning. Hence, an object of volScalarField must be defined in the constructor and the initial values must be defined in 0 folder. Also it must be written in the harddisk with the other results when it is commanded to be written by the user. So that, simulation can be stopped and started again.

```
template<class BasicPsiThermo, class MixtureType>
void Foam::heRhoThermo<BasicPsiThermo, MixtureType>::correct()
{
if (debug)
{
Info<< " Corrected" << endl;
}
const volVectorField& U = this->db().objectRegistry::lookupObject
<volVectorField>("U.particles");
volScalarField TR = sqrt(2.0)*mag(symm(fvc::grad(U)));
calculate(TR);
if (debug)
{
Info« " Finished" « endl;
}
}
```

New viscosity model implementation in bloodTransportI.H file is shown below;

```
template<class Thermo>
inline Foam::scalar Foam::bloodConstTransport<Thermo>::mu
(
const scalar p,
const scalar T, const scalar alpha1, const scalar sr
) const
{
...
//Calculations of the viscosity of RBCs are done here. This model can be
different due to the viscosity model.
...
}
```

APPENDIX A.2 - Implementation details of Wall Shear Stress and Spatial Wall Shear Stress Gradient for two-phase flow in OpenFOAM

Wall Shear Stress (WSS) and Spatial Wall Shear Stress Gradient (SWSSG) calculations are implemented in OpenFOAM as a postprocess function such as wallShearStress utility of OpenFOAM. wallShearStress utility is already coded in OpenFOAM however in two-phase flow, some modifications are required to obtain WSS.

Reff value which is needed to calculate WSS, called from turbulence model in OpenFOAM. If there is no turbulence model in the simulation, WSS can not be calculated. Also the transport properties of RBCs vary due to shear rate and volume fraction. Therefore, wallShearStress utility is extended to get WSS and SWSSG for twoPhaseEulerFoam. Author encountered that even if the turbulence model is used for both cases, for example kinetic theory RAS model for RBCs and k-epsilon for plasma, wallShearStress gives an error which says that is unable to find turbulence model. That's why Reff calculations are modified in the first place. Generel form of the equation is,

```
Reff = -nu_ * dev(twoSymm(fvc::grad(U)));
```

In order to calculate viscosity, nu, of RBCs, shear rate and volume fraction are required. IO objects are created to read and attain these values. After obtaining "nu" value of the mixture, wall shear stress calculation function is called.

```
calcShearStress(mesh, Reff(), wallShearStress);
```

With the calculated Wall Shear Stress value, SWSSG value can also be calculated.

```
volTensorField gradWSS = fvc::grad(shearStress);
forAllConstIter(labelHashSet, patchSet_, iter)
{
label patchi = iter.key();
tensorField& gradW = gradWSS.boundaryFieldRef()[patchi];
scalarField& ssg = SWSSG.boundaryFieldRef()[patchi];
const vectorField& Sfp = -mesh.Sf().boundaryField()[patchi];
const scalarField& magSfp = mesh.magSf().boundaryField()[patchi];
vectorField beta = (Sfp / magSfp)^alpha;
ssg = mag(diag(gradW));
}
SWSSG.write();
```

CURRICULUM VITAE

Name Surname: Utkan Çalışkan

Place and Date of Birth: Rize, 02.01.1992

Adress: Istanbul Technical University, Institute of Informatics, Department of Computational Science and Engineering

E-Mail: caliskanutkan@gmail.com

B.Sc.: Mechanical Engineering, Istanbul Technical University

M.Sc.: Computational Science and Engineering

Professional Experience and Rewards:

List of Publications and Patents:

PUBLICATIONS/PRESENTATIONS ON THE THESIS